

THE PETROLOGY, GEOCHEMISTRY, AND FLUID HISTORY OF CALC-SILICATE  
ROCKS AND ASSOCIATED PRIMARY Cu-Co MINERALIZATION IN THE  
ETHIUDNA MINES AREA, OLARY PROVINCE, SOUTH AUSTRALIA.

Benjamin Grguric, BSc.

Thesis submitted as partial fulfilment of the  
Honours Degree of Bachelor of Science

Department of Geology and Geophysics,  
University of Adelaide

November, 1992

NATIONAL GRID REFERENCE : PLUMBAGO SHEET 6833 (1:63,360)

COPY 2

## TABLE OF CONTENTS

CHAPTER 1	
INTRODUCTION.....	1
1.1. INTRODUCTION.....	1
1.2. HISTORY AND PREVIOUS INVESTIGATIONS.....	1
1.3. AIMS AND METHODS OF STUDY.....	2
CHAPTER 2	
GEOLOGICAL BACKGROUND.....	3
2.1. REGIONAL GEOLOGY AND STRATIGRAPHY OF THE WILLYAMA SUPERGROUP.....	3
2.2. STRATIGRAPHY OF THE ETHIUDNA SUB-BLOCK.....	5
2.2.1. Biotite Microclinolite.....	5
2.2.2. Metapelites.....	6
2.2.3. Ethiudna Adamellite.....	6
2.3. STRUCTURAL GEOLOGY OF THE ETHIUDNA SUB-BLOCK.....	7
2.4. METAMORPHISM OF THE ETHIUDNA SUB-BLOCK.....	8
CHAPTER 3	
PETROLOGY AND FLUID HISTORY OF THE BIMBA SUITE.....	10
3.1. INTRODUCTION.....	10
3.2. PETROGRAPHY OF THE BIMBA SUITE.....	10
3.2.1. The Wollastonite-Diopside Subunit.....	10
3.2.2. The Calc-Silicate Quartzite.....	11
3.2.3. The Footwall Quartzite.....	12
3.3. PETROGENESIS OF THE BIMBA SUITE.....	12
3.3.1 Description of textures.....	12
3.3.2 Interpretation of textures implications for fluid infiltration.....	13
3.4. AQUEOUS ELECTROLYTE COMPOSITIONS OF METASOMATIC FLUIDS.....	16
3.4.1. Fluid inclusion analysis.....	16
3.4.2. Scapolite analysis.....	18
3.4.3. Origin of high metamorphic fluid salinities.....	21
3.5 CARBON-OXYGEN STABLE ISOTOPE GEOCHEMISTRY OF THE BIMBA SUITE.....	21
CHAPTER 4	
SULPHIDE PETROLOGY AND GENESIS.....	25
4.1. THE NATURE AND DISTRIBUTION OF PRIMARY SULPHIDE MINERALIZATION.....	25
4.1.1. Ethiudna mines.....	25
4.1.2. Ethiudna East prospect.....	26
4.1.3. Other sulphide occurrences.....	26
4.2. ORE TEXTURES AND MINERALOGY.....	27

4.3. DISTRIBUTION AND STRUCTURAL CONTROL OF  
MINERALIZATION  
    GENETIC IMPLICATIONS .....3 0  
4.4. GENESIS OF STRATA-BOUND Cu-Co MINERALIZATION.....3 1  
4.5. EVIDENCE FOR METASOMATIC REMOBILIZATION OF  
MINERALIZATION .....3 3

ACKNOWLEDGEMENTS

REFERENCES

APPENDIX 1: WHOLE ROCK ANALYSES  
APPENDIX 2: CARBON-OXYGEN ISOTOPE ANALYSES  
APPENDIX 3: MICROPROBE ANALYSES-SCAPOLITE  
APPENDIX 4: MICROPROBE ANALYSES-SULPHIDES  
APPENDIX 5: FLUID INCLUSION ANALYSES  
APPENDIX 6: SULPHUR ISOTOPE ANALYSES  
APPENDIX 7: UNIVARIANT REACTIONS AND SLOPES OF UNIVARIANT LINES

## LIST OF FIGURES

- Figure 1 Location of the study area.
- Figure 2 Schematic stratigraphy of the Willyama Supergroup metasediments in the study area, and regional correlations.
- Figures 3a and 3b Discriminant diagrams for altered volcanics and volcanoclastics.
- Figure 4 XCO<sub>2</sub>-T diagram showing univariant curves for the reaction calcite + quartz => wollastonite + CO<sub>2</sub>.
- Figure 5  $\mu$ K<sub>2</sub>O- $\mu$ CO<sub>2</sub> diagram for the system KCASH.
- Figure 6 Histograms of data from microthermometric measurements on fluid inclusions.
- Figure 7 Compositions of Ethiudna scapolites.
- Figure 8 Correlations between scapolite composition and fluid composition.
- Figure 9 Carbon-oxygen isotope profiles.
- Figure 10 Sulphide species proportions: stratigraphic variation.
- Figure 11 T-X diagram for phase relations in the system Fe-S.
- Figure 12 Ternary plot of Ethiudna pyrite compositions.
- Figure 13 Histogram of sulphur isotope analyses.
- Figure 14 Drill hole assay profiles.

## LIST OF TABLES

- Table 1 Modal compositions of Ethiudna microclinolites.
- Table 2 Wollastonite Stage assemblages.
- Table 3 Carbon-oxygen isotope analyses.
- Table 4 Mineralogy of sulphide mineralization.
- Table 5 Geochemical characteristics of Ethiudna mineralization.

## LIST OF PLATES

- Plates 1-6 Photographs and photomicrographs displaying textural relationships in calc-silicates.
- Plates 7-8 Photomicrographs of fluid inclusions.
- Plates 9-17 Photomicrographs of ore textures.



## ABSTRACT

Textures in calc-silicate rocks of the Lower Proterozoic Bimba Suite in the Ethiudna mines area, Olary Province, South Australia, record multiple fluid infiltrational episodes associated with both prograde, amphibolite-facies, and retrograde, greenschist-facies metamorphism. Pervasive infiltration of H<sub>2</sub>O-rich fluids ( $X_{CO_2} < 0.18$ ) during prograde metamorphism, was associated with the large-scale development of wollastonite-rich lithologies within the Bimba Suite. Stable oxygen isotope evidence suggests these fluids were equilibrated with a siliciclastic sequence(s) prior to infiltrating the Bimba Suite.

A second, retrograde metamorphic (temperatures  $\sim 300^\circ\text{C}$ ) infiltrational episode was associated with the development of a grossular-quartz assemblage. Fluid flow was channelized during this episode, the H<sub>2</sub>O-rich fluids being focussed along structurally-induced zones of high permeability. Large variations in fluid/rock ratios are recorded in the calc-silicates as large variations in the progress of the grossular-quartz producing reaction.

The formation of cross-cutting quartz, calcite, and rare laumontite veins postdates both these infiltrational episodes. Fluid inclusion evidence suggests these veins were deposited by fluids at temperatures of less than  $250^\circ\text{C}$ .

Fluid inclusion data and scapolite compositional data indicate fluids associated with all three episodes were highly saline, consistent with conclusions made by earlier workers that the Bimba Suite represents a meta-evaporite sequence.

The microcline-rich rocks of the Quartzofeldspathic Suite, which underlies the Bimba Suite, host stratiform and disseminated Cu-Co sulphide mineralization. Geochemical and petrological evidence suggests this mineralization is of the genetic type known as a red-bed-associated Cu deposit. The distribution, geochemistry, and textural characteristics of sulphides in the Bimba Suite, suggest this mineralization represents a metasomatic remobilization of pre-metamorphic Quartzofeldspathic Suite mineralization. The sulphide-silicate-carbonate textural relationship in the Bimba Suite suggests this remobilization took place during the high temperature, wollastonite-producing infiltrational episode, and that precipitation of ore metals was effected by a pH rise.

## CHAPTER 1 : INTRODUCTION

### 1.1. INTRODUCTION

Fluids attending regional and contact metamorphism have long been recognized as a necessary component for the formation of many calc-silicate minerals in impure carbonate rocks. They have also been implicated as potential transporting agents of ore elements, and their involvement in the formation of skarns and greenstone-type Au deposits is well documented (Einaudi et al., 1981; Golding et al., 1990). This thesis documents a study into the role of fluids in high temperature metamorphism and mineralization of calc-silicates in the Ethiudna mines region of the Olary Province, S.A. The Ethiudna mines area provides a suitable location for an investigation into such processes since unusual Cu-Co sulphide mineralization is known to occur within a sequence of wollastonite-bearing calc-silicate rocks, the presence of the latter suggesting the possibility of high temperature metasomatism.

### 1.2. HISTORY AND PREVIOUS INVESTIGATIONS

The Ethiudna mines are located in a low range of outcropping crystalline rocks approximately 5kms W of Plumbago Homestead, and some 55kms NNE of Mannahill in the Olary Province of South Australia (Fig.1). The mines, together with numerous other small occurrences of copper, cobalt and graphite in the area were worked sporadically between 1889 and 1914 for their rich but short-lived secondary ores. Mineralization at the Ethiudna mines was investigated by the S.A. Department of Mines in the 1950's, their mapping and diamond drilling program resulting in the discovery of the Ethiudna East prospect which proved however, to be subeconomic (Campana & King, 1958). Cursory exploitation of secondary copper ores was carried out by Petrocarb in the 1960's, and the Ethiudna area was the subject of a structural/metamorphic geology honours thesis by Waterhouse (1971). In the 1980's the mines came under investigation by Adelaide Chemical Co. as a potential economic source of

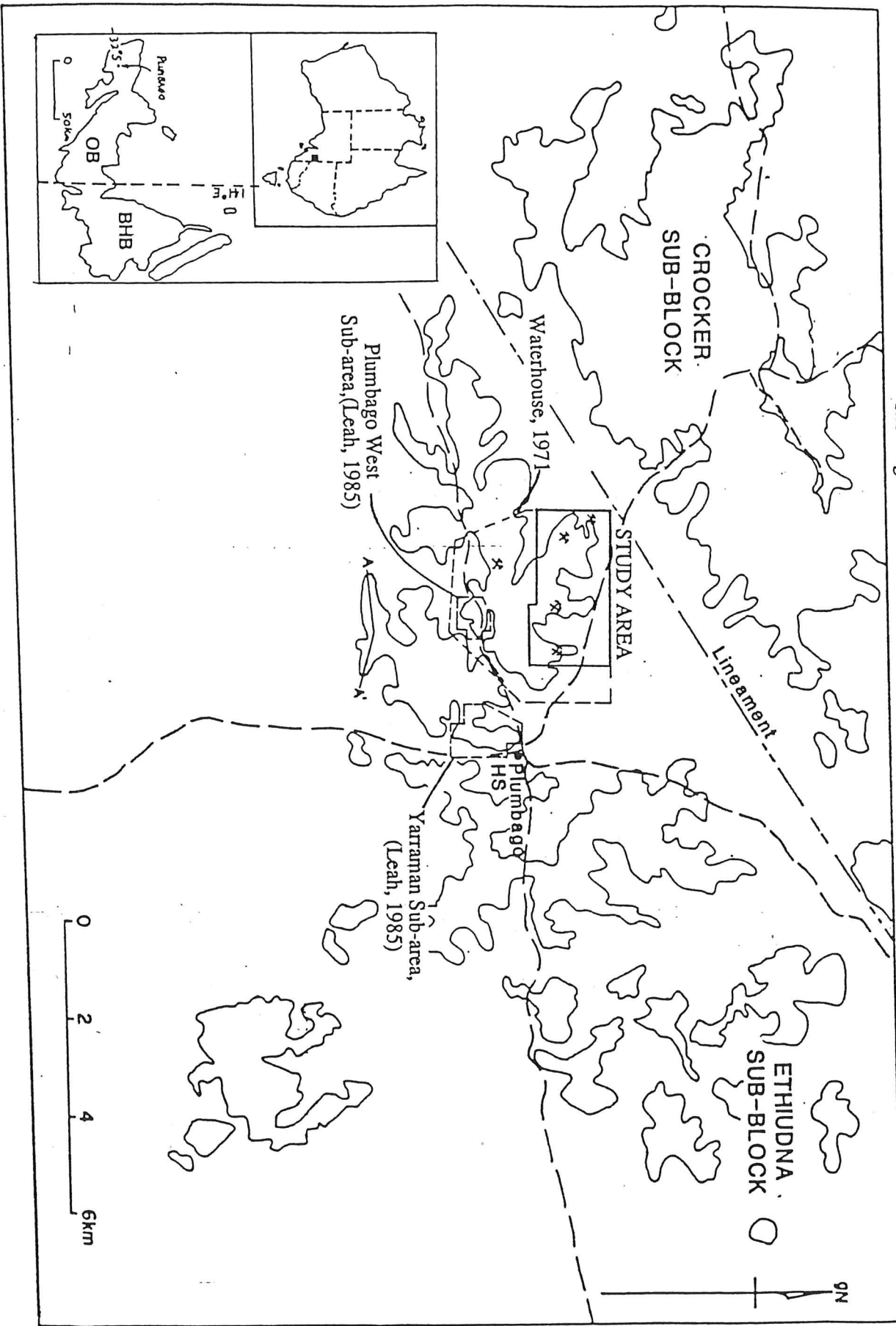


Figure 1: Map of basement outcrop in the Plumbago area (after Leah, 1985), showing the location of the study area and previous study areas.

140° 00' 32" 00'

the industrial mineral, wollastonite. The area is still under consideration by this company, whose resource evaluation program has resulted in upwards of twenty diamond drill cores being available.

### 1.3. AIMS AND METHODS OF STUDY

The primary aims of this project are: (1) to define the processes which produced the calc-silicate assemblages and textures observed in the Bimba Suite at Ethiudna; (2) establish whether infiltrational metasomatism has occurred, and if so, to further establish how many episodes of fluid infiltration occurred during metamorphism of the sequence, the chemical compositions of the fluids associated with each episode, and whether fluid flow was pervasive or channelized; and (3) to determine the nature and origin of primary mineralization present in the metasediments, and the effects of metamorphism and metasomatism on the sulphide assemblages.

In order to achieve these aims, standard petrological and geochemical techniques were applied. The methods used included; (1) detailed mapping and sampling of an area 2.75 x 1.5km; (2) examination of 33 polished thin sections and 10 polished blocks; (3) bulk rock XRF analyses of 18 samples for both major and trace elements; (4) electron microprobe analyses of; 113 sulphides and arsenides (WDS), 30 scapolites (WDS), 150+ calc-silicate minerals (EDS); (5) utilization of X-ray diffraction and SEM-EDAX semi-quantitative analysis for the identification of mineral grains; (6) microthermometric measurements on 16 fluid inclusions; (7) sulphur isotope analyses of 31 sulphide samples; (8) carbon-oxygen isotope analyses of 20 calcite samples and one carbon isotope analysis of graphite. In addition, core logs, geophysical data and drill hole assays from Adelaide Chemical Co.'s wollastonite exploration program provided by K.F. Bampton, were examined.

## CHAPTER 2 : GEOLOGICAL BACKGROUND

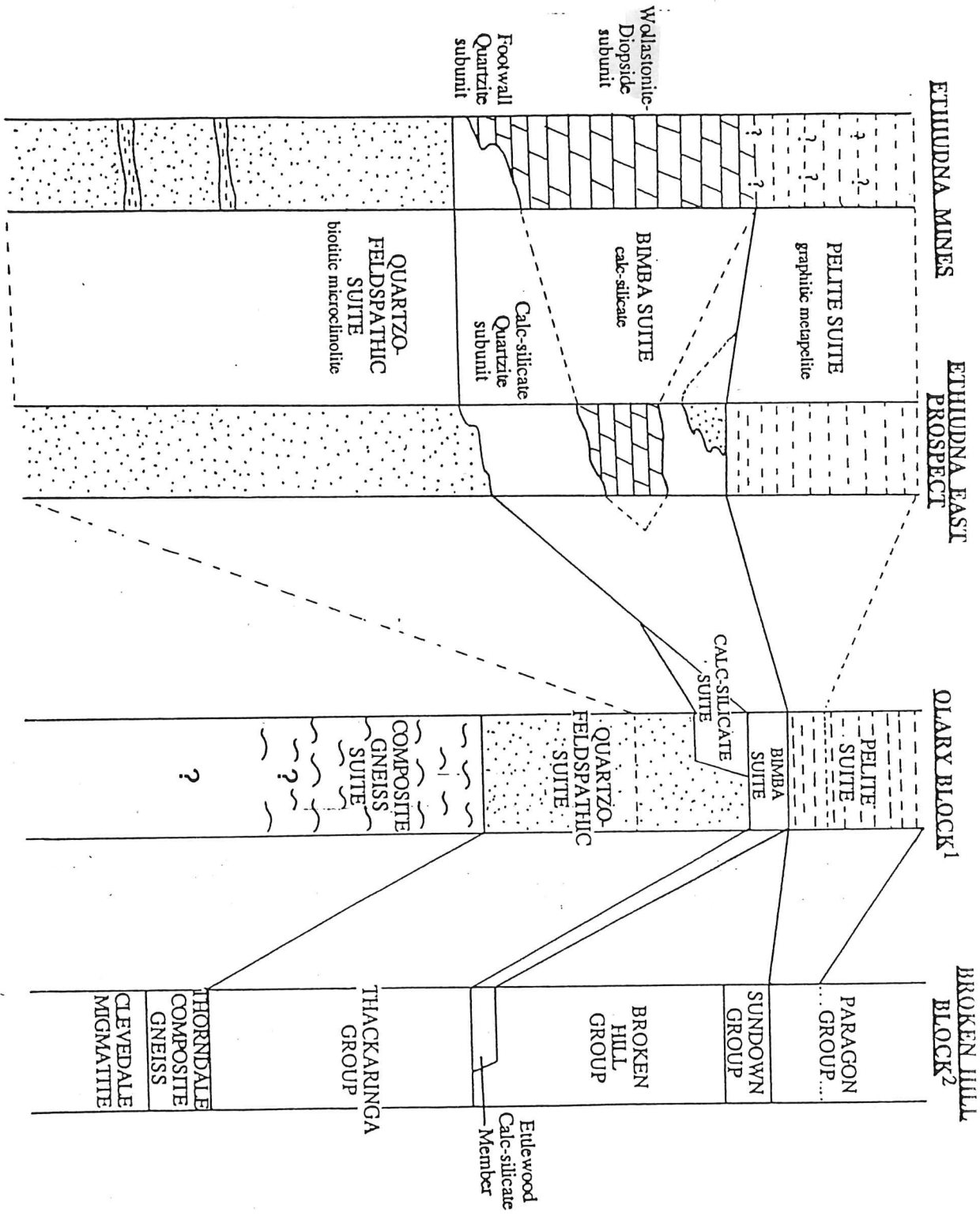
### 2.1. REGIONAL GEOLOGY AND STRATIGRAPHY OF THE WILLYAMA SUPERGROUP

The outcropping metasediments of the Ethiudna area comprise part of the Lower Proterozoic Willyama Supergroup (WS), a polydeformed basement sequence which is subdivided into the Olary Block (OB) and the Broken Hill Block (BHB), west and east of the S.A./N.S.W. border, respectively. Late Proterozoic Adelaidean metasediments, which unconformably overlie this sequence, are widely exposed in the OB but are not present in the mapped area.

The stratigraphy of the mapped area based on outcrop and drill core information is shown in Fig.2. The calc-silicate subunits collectively known as the Bimba Suite (Clarke et al., 1986), are underlain by microclinolites of the Quartzofeldspathic Suite and overlain by graphitic pelites of the Pelite Suite. The Bimba Suite shows considerable variation in thickness within the mapped area, and is noticeably absent in the eastern quarter of the mapped area.

Considerable variation in the mineralogy and bulk chemistry of the Bimba Suite occurs in the Willyama domain, reflecting a combination of original sedimentary compositional variation and differing styles and grades of metamorphism. Thick beds of wollastonite within the unit are unique to the Ethiudna area; elsewhere in the OB this mineral is present only as a rare accessory phase (Cook & Ashley, 1992).

A similar stratigraphy is seen throughout the OB, and a strong correlation exists with BHB metasediments (Fig.2), although albitites are more common than microclinolites in both subdomains (Clarke et al., 1986; Cook & Ashley, 1992).



A volcanically active, marine, ensialic rift has previously been proposed for the depositional environment of the WS (Stevens et al., 1980; Willis et al., 1983), however recent boron isotope studies by Slack et al. (1989), suggest stratiform tourmalinites within the Supergroup were derived from non-marine borates, thus implying a continental rift setting. In this setting, the Bimba Suite and its BHB equivalent, the Etlewood Calc-Silicate, are suggested on the basis of sedimentological and geochemical evidence, as representing a carbonate/evaporite sequence deposited in a hypersaline (playa) environment (Cook & Ashley, 1992). Metallogenetic processes were an integral part of WS rift sedimentation and epigenesis as exemplified by the giant Broken Hill orebody (Both & Rutland, 1976), banded iron formations on Plumbago, and numerous occurrences of stratiform Cu-Co mineralization (Campana & King, 1958).

The sediments of the WS were metamorphosed and intensely deformed during the middle Proterozoic 'Olarian Orogeny'. Clarke et al. (1986), described three deformation events (D1-D3) that occurred during this orogeny. The D1 event produced meso- to macroscopic, isoclinal, recumbent, NE to E-trending F1 folds, which were overprinted during D2 by tight to open, upright, NE to E-trending F2 folds. Development of a near-vertical S2 schistosity in pelitic rocks resulted in the crenulation and local obliteration of earlier bedding-parallel S1 fabrics. Gentle warping of preexisting fabrics by E-trending F3 folds, and the development of retrograde shear-zones characterize the D3 event.

Prograde metamorphism and the regionally extensive intrusion of granitoids was associated with the D1 and D2 events, with peak metamorphic conditions generally being attained late in D2 (Clarke et al., 1987). Marked variation in grade of peak metamorphism occurred across the Willyama domain during the Olarian Orogeny, ranging from granulite facies in the BHB, to upper greenschist facies in the northern OB. Retrograde metamorphism associated with the D3 event and the Cambrian/Ordovician Delamerian Orogeny is generally of greenschist-facies grade (Clarke et al., 1987). The structural response of the Willyama

basement to the latter event is limited to minor regional warping of the basement blocks, and the development of mylonite zones (Clarke et al., 1986).

## 2.2. STRATIGRAPHY OF THE ETHIUDNA SUB-BLOCK

The petrography of non-calc-silicates which dominate the outcrop in the study area are briefly described below. The petrology and petrography of calc-silicates is described in detail in Chapter 3.

### 2.2.1. Biotite Microclinolite

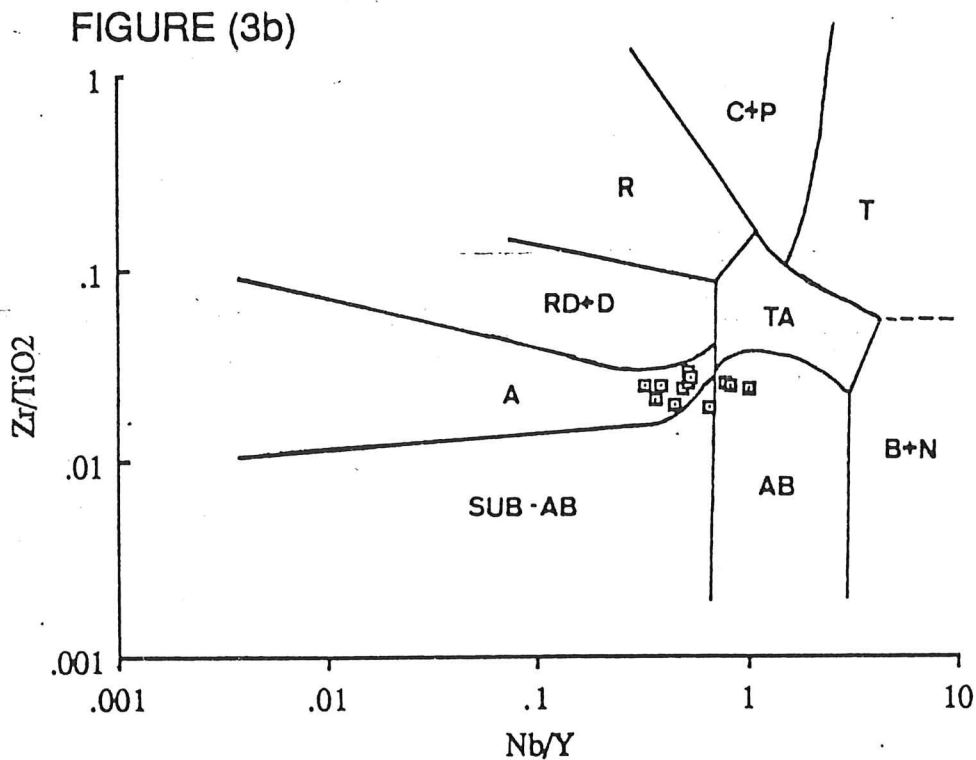
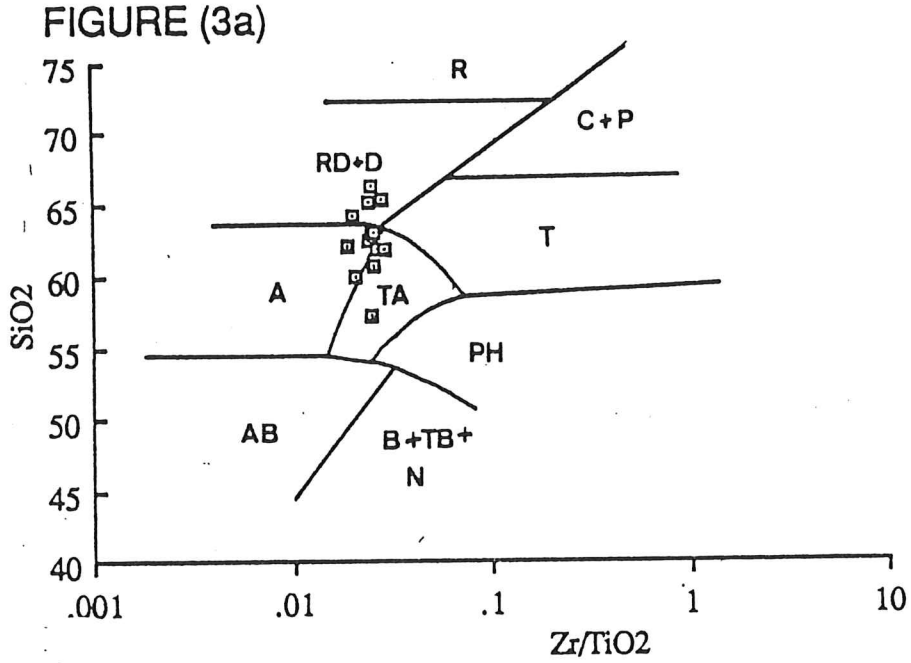
This lithology, representing the uppermost section of the Quartzofeldspathic Suite, outcrops extensively in the Ethiudna Sub-Block. It consists primarily of fine to medium-grained microcline, biotite, and quartz with variable proportions of albite, hematite, and accessory titanite (Table 1). Locally, the unit hosts stratiform and disseminated sulphide mineralization (vide chapter 4). Moderate to well developed layering is present in the microclinolites and is defined by grainsize variation, and variation in the modal abundance of biotite. The presence of relict graded bedding within layers suggests this layering to be a primary feature. Gradation of the microclinolites into migmatites is common in the vicinity of adamellite bodies, and the unit is extensively intruded by boudinaged and ptygmatically-folded, syntectonic pegmatites associated with the granitoids.

Models incorporating the mechanisms of Coombs (1965), and Surdam and Parker (1972), have been favoured by workers investigating the petrogenesis of OB microclinolites and similar albitites (Plimer, 1977; Ashley, 1984; Leah, 1985), since the major element composition of these lithologies do not conform to that of any primary igneous or sedimentary rock. These models involve the alteration or areally extensive airfall tuffs and their reworked equivalents to analcime-rich sediments under hypersaline (playa) conditions. Growth of authigenic albite (or microcline) at the expense of analcime is attributed to subsequent



TABLE (1): Modal composition of Ethiudna microclinolites.

MINERAL	AVERAGE %	RANGE %
microcline	65	10 - 85
quartz	12	5 - 80
albite	10	5 - 55
biotite	9	3 - 30
hematite	3	0 - 8
titanite	1	0 - 2



FIGURES (3a). and (3b): Immobility trace element data from Ethiudna microclinolites superimposed on discrimination diagrams for altered volcanics and volcanoclastics (after Floyd and Winchester, 1978).

R= rhyolites; C+P= comendites and pantellerites; RD+D= rhyodacites and dacites; T= trachytes; A= andesites; TA= trachyandesites; PH= phonolites; AB= alkali basalts; SUB-AB= sub-alkaline basalts; B+TB+N= basanites, trachybasanites, nephelinites.

diagenesis of the sediments. Application of immobile trace element data from Ethiudna microclinolites to discriminant diagrams for altered volcanics and volcanoclastics (after Floyd & Winchester, 1978), suggests a felsic to intermediate tuffaceous progenitor (Figs. 3a and 3b).

### 2.2.2. Metapelites

The dominant pelitic lithology in the study area is a well-laminated, locally graphitic biotite schist containing prominent sericite porphyroblasts up to 2cm in diameter. The mineralogy of these pelites comprises medium-grained biotite, muscovite, sericite, quartz, with lesser cordierite, fibrolitic sillimanite and locally developed euhedral chloritoid. The graphite content of this lithology is highly variable along strike (5-85%), and is suggested on the basis of its isotopic composition ( $\delta^{13}\text{C} = -29$  per mil), to be of organic origin (D. McKirdy, pers. comm.).

### 2.2.3. Ethiudna Adamellite

The syn-tectonic Ethiudna Adamellite and associated pegmatites account for approximately two thirds of the total outcrop in the study area. The adamellite is coarse-medium grained, homogeneous, and comprised of large (1.5-4cm), euhedral, microcline phenocrysts in an equigranular matrix consisting of microcline, andesine, quartz, biotite and muscovite. Associated pegmatites are widespread, and are characterized by locally graphitic microcline, albite, quartz and accessory schorl and ilmenorutile. Metasedimentary xenoliths are common, and are predominantly microclinolites and pelites identical to those outcropping in the study area.

The normative composition of the Ethiudna Adamellite implies the granitoid is a true adamellite (Leah, 1985). Chemical characteristics of the adamellite, namely high  $\text{SiO}_2$ , low CaO and a  $\text{Al}_2\text{O}_3/(\text{Na}_2\text{O}+\text{K}_2\text{O}+\text{CaO}) > 1.1$  ( $=1.25$ ; Leah, 1985) imply it to be an S-type granitoid according to the classification scheme of Chappell and White (1974). The relatively

high Ba, Rb, Zr, La, Ce and Y content of the granitoids (with respect to S-type parameters) is suggested to reflect the assimilation of late-stage differentiated volcanoclastics in the metasedimentary source region (Ashley, 1984).

### 2.3. STRUCTURAL GEOLOGY OF THE ETHIUDNA SUB-BLOCK

The structural geology of the Ethiudna Sub-Block is complex, reflecting the overprinting of several deformation episodes. The structural features which characterize each recognizable deformational event (D1-D3), are briefly outlined below. Based on the nature of their associated structures, events D1-D3 are correlated with the regional Olarian D1-D3 events (after Clarke et al., 1986) described above.

The Olarian D1 event is represented in WS metasediments of the Sub-Block by macroscopic, isoclinal, recumbent, E-trending folds (F1). An axial planar S1 fabric is defined by phyllosilicates and parallels lithological layering, except in fold closures (Waterhouse, 1971; Leah, 1985). D2 structures dominate the metasedimentary terrain of the Ethiudna Sub-Block. Previous work has shown the study area lies on the NW limb of a macroscopic, NE-trending, F2 antiform, the core of which has been extensively intruded by the Ethiudna Adamellite (Campana & King, 1958; Waterhouse, 1971). Mesoscopic F2 folds within the study area are tight to open, upright or slightly inclined to the S, and trend E to NE. A strongly developed axial planar S2 fabric, which crenulates, and commonly obliterates S1, is prevalent within pelites and microclinolites. The intrusion of the voluminous Ethiudna Adamellite is suggested to have occurred during the D2 event, as evidenced by;

- a) the presence of a weak planar fabric parallel to S2 in the granitoids defined by the alignment of biotite laminae and microcline phenocrysts.
- b) the occurrence of boudinaged pegmatites associated with the granitoids; the principal elongation direction of boudinage being parallel to F2 trends.

D3 in the study area is represented by non-pervasive, open, NE-trending mesoscopic flexures. A weak S3 fabric is developed in pelites defined by retrograde sericite. Minor NE-SW trending faults recording only small displacement occur in the Ethiudna area which cross-cut all earlier developed structures.

#### 2.4. METAMORPHISM OF THE ETHIUDNA SUB-BLOCK

Metamorphism in the Ethiudna Sub-Block has previously been investigated by Waterhouse (1971), and Leah (1985), their studies being focussed on pelite assemblages. The interpreted metamorphic history of the Sub-Block, based on observations made by the author and these previous workers, is summarized below.

The S1 foliation is defined in the study area by the assemblage biotite-muscovite± actinolite, which poorly constrains P,T conditions associated with the D1 event. M1 porphyroblasts in pelites, around which S2 biotite and muscovite are wrapped, are pervasively pseudomorphed by retrograde sericite, and therefore provide little unequivocal constraint on the metamorphic conditions prevailing during D1. Elsewhere in the western region of the OB, these porphyroblasts are andalusite (Clarke et al., 1987).

Peak metamorphism of amphibolite-facies grade coincided with the Olarian D2 event as evidenced by the presence of the assemblage sillimanite-cordierite-muscovite defining S2 in pelites (Waterhouse, 1971). Elevated temperatures (>550°C) are implied by the presence of sillimanite, while muscovite stability precludes temperatures much in excess of 650°C. The elevated temperatures may reflect the abundant syn-D2 intrusions of adamellite in this area. The presence of cordierite and the absence of kyanite, staurolite and almandine in S2 implies pressures were not greater than about 3-4kbar during the peak event.

Retrograde metamorphism was associated with the D3 event, as evidenced by the presence of sericite and rare biotite defining S3 in pelites and microclinolites. The growth of

post-sericitization chloritoid porphyroblasts in pelites has been suggested as occurring during a mild thermal event ( $<500^{\circ}\text{C}$ ) associated with D3 or the Delamerian Orogeny (Leah, 1985).

## CHAPTER 3 : PETROLOGY AND FLUID HISTORY OF THE BIMBA SUITE

### 3.1. INTRODUCTION

Calc-silicate phase equilibria provide useful petrogenetic information with which the fluid history of a metamorphic terrain can be characterized, owing to the fact that the reactions involved are frequently highly dependent on the composition of the attending fluid phase. Studies of the stable isotopic composition of metamorphic carbonates can also shed light on the extent of fluid/rock interaction, during fluid flow events (Bickle & Baker, 1990).

Investigations into fluid processes associated with metamorphism were centred on the Bimba Suite at Ethiudna since the predominance of both calc-silicates and carbonates within the unit allowed both petrological and stable isotopic methods to be implemented. For the purposes of mapping and drill-core interpretation, the Bimba Suite has been divided into three texturally and mineralogically distinct subunits; viz. the Wollastonite-Diopside subunit, the Calc-Silicate Quartzite, and the Footwall Quartzite. The characteristics of each subunit and the observed textures and phase relationships of its mineral assemblages will be discussed in turn, in order to provide the basis for a detailed interpretation of the high temperature significance of the calc-silicates.

### 3.2. PETROGRAPHY OF THE BIMBA SUITE

#### 3.2.1. The Wollastonite-Diopside Subunit

This subunit is characterized by the component minerals, wollastonite, diopside, calcite, quartz and microcline with localized development of grossular and vesuvianite. Accessory titanite, apatite and sulfides are ubiquitous. Marked layering is developed in the subunit, defined by differences in the modal abundance of component minerals, and is prominent in outcrop due to preferential weathering of calcite-rich layers. This layering is

interpreted as essentially primary in origin with local accentuation due to metamorphic segregation. Such a hypothesis is supported by; a) the persistence of individual layers less than 2cm thick over distances of 10 metres or more (Waterhouse, 1971), and b) the conformity of the layering with that of the underlying Calc-Silicate Quartzite and Quartzofeldspathic Suite in which relict sedimentary structures are preserved.

Mineralogically the unit is dominated by wollastonite and diopside, which in the case of wollastonite may comprise more than 70% of layers totalling several metres in thickness. Layers of marble are common in the subunit, reaching a maximum observed thickness of 2 metres at the Ethiudna East prospect. These marbles are remarkable for their purity, averaging less than 3% of other phases, notably wollastonite and sulphides.

### 3.2.2. The Calc-Silicate Quartzite

The major part of outcropping Bimba Suite calc-silicate rocks within the Ethiudna Sub-block is represented by this subunit, which consists predominantly of quartz with well-developed fine layering defined by diopside, epidote, mizzonitic scapolite and locally, hornblende and actinolite. The relative proportion of calcite present within the lithology shows marked variation along strike. Local increases in the modal abundance of calcite from 1-2% up to 15-40% correspond with the development of the overlying Wollastonite-Diopside subunit. Such carbonate-rich zones as exemplified by the Ethiudna East prospect are characterized by the abundance of disseminated sulphides and the extensive development of clinozoisite, grossular, and epidote. Rare boudins of both pure diopside and mizzonite were observed enclosed in calcite-poor layers of the subunit in the vicinity of the prospect, with the latter type reaching up to 50 cms in length. The principal elongation direction of the boudins is parallel to the trend of lithological layering suggesting formation by metamorphic segregation.

### 3.2.3. The Footwall Quartzite

This unit is limited in outcrop to the Ethiudna mines area where its stratigraphic position between the microclinolites of the Quartzofeldspathic Suite and the Wollastonite-Diopside subunit suggests correlation with the Calc-Silicate Quartzite. The two subunits differ essentially only in the lower calc-silicate content of the Footwall Quartzite and its higher microcline content. The subunit consists of a feldspathic quartzite with a variable calc-silicate component consisting of diopside, andradite, wollastonite, and lesser grossular and calcite. Chlorapatite and titanite are a common accessory, and calc-silicate-rich zones are also frequently host to disseminated sulphides. The contact between this subunit and the overlying Wollastonite-Diopside subunit is always gradational, defined by the increasing modal abundance of wollastonite upsection or involves intercalation of the two subunits over a scale of less than 1 metre.

## 3.3. PETROGENESIS OF THE BIMBA SUITE

### 3.3.1 Description of textures

The observed textures and mineralogy of the Bimba Suite are complex reflecting the influence of variable bulk compositions in combination with a complex polymetamorphic history possibly involving multiple fluid infiltration events. Notwithstanding the textural complexity, it is evident that the rocks have undergone several discrete events resulting in textural and mineralogical modification. Characteristic assemblages were recognized as being associated with three such events, named in order of their observed paragenetic position in the petrogenesis of the Wollastonite-Diopside subunit. The textural and mineralogical features which characterizes each of these stages will be discussed in turn.

The Wollastonite Stage: This stage is characterized by assemblages containing wollastonite together with combinations of diopside, calcite, microcline and quartz (Table 2). These



assemblages define a coarse-grained, granoblastic fabric and are in apparent textural equilibrium as indicated by triple point junctions between phases.

The Grossular Stage: This stage is characterized by the appearance of grossular together with a second generation of quartz as localized replacements of the previously developed microcline-wollastonite association. Varying degrees of replacement are observed ranging from thin grossular-quartz rims along microcline-wollastonite grain boundaries to relatively pure quartz-grossular rock, implying in the latter case complete replacement of the earlier formed assemblage. The occurrence of this grossular-quartz rock is restricted to fold hinges at the Ethiudna East prospect.

The Brittle-Fracture Stage: Veins of quartz, calcite, and rare laumontite, which are locally present in all Bimba Suite subunits characterize this stage. These veins cross-cut, and therefore post-date, assemblages of the previous two stages.

### 3.3.2 Interpretation of textures: implications for fluid infiltration

Several reactions have been proposed in order to account for the textures observed in the aforementioned stages. Wollastonite in the Wollastonite-Diopside subunit is suggested as originating via the reaction;



based on the abundance of presumably unreacted quartz and calcite (grains of these two minerals were never observed in direct contact with each other) within the subunit, and the lack of textural evidence suggesting its origin via other wollastonite-producing reactions.

For a given pressure, the temperature at which this reaction occurs is highly dependent in the molar fraction of CO<sub>2</sub>, (or X<sub>CO2</sub>) in the attendant fluid phase (Fig. 4). The shaded area on Fig. 4 shows the maximum values of X<sub>CO2</sub>(fluid) in which wollastonite could have

wollastonite - diopside - calcite - microcline
wollastonite - diopside - quartz - microcline
wollastonite - diopside - calcite
wollastonite - diopside - quartz
wollastonite - diopside - microcline
wollastonite - calcite
wollastonite - quartz
wollastonite - diopside
wollastonite - microcline

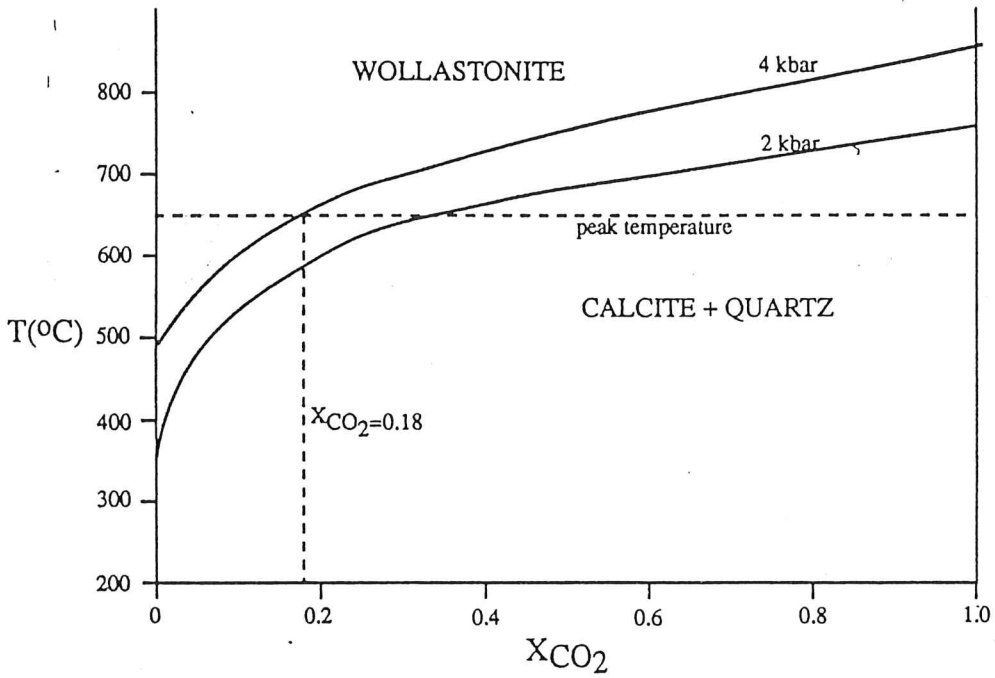


FIGURE (4):  $X_{CO_2}$ - $T$  diagram showing univariant curves for reaction (1) at 2 and 4 kbars (after Greenwood, 1967; and Schenk, 1984). Explanation in text.

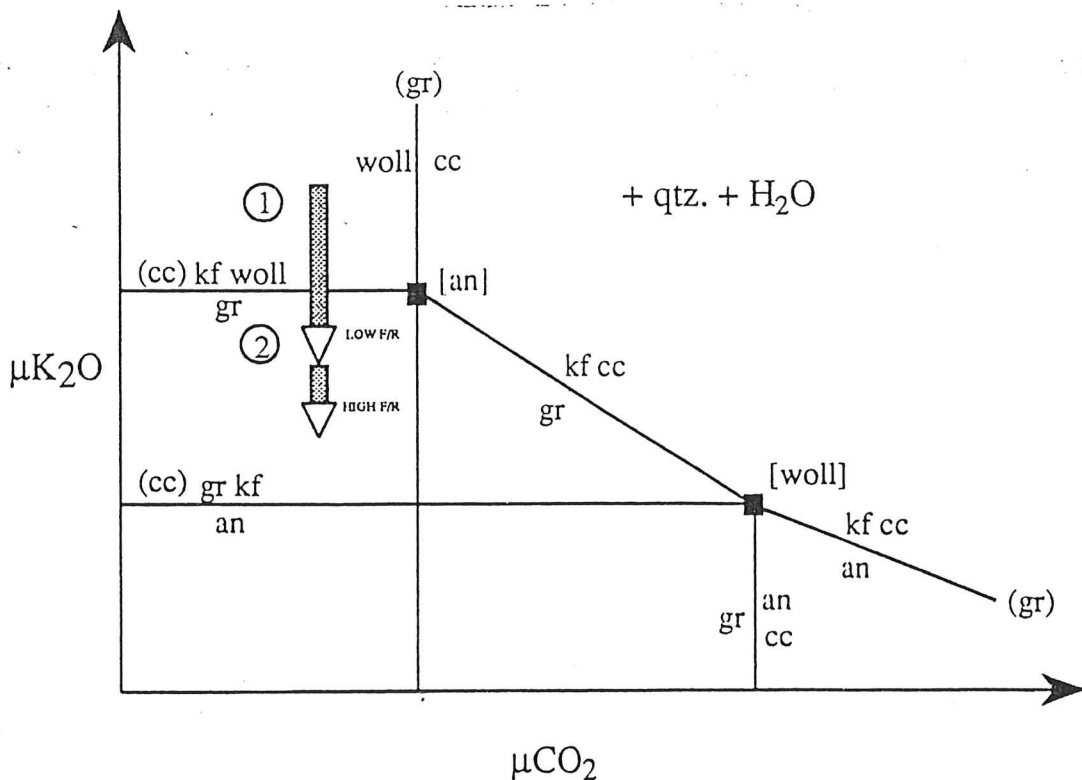
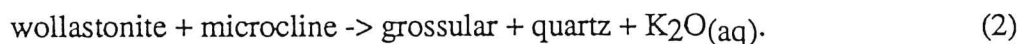


FIGURE (5):  $\mu_{K_2O}$ - $\mu_{CO_2}$  diagram qualitatively showing phase relationships for the system KCASH relevant to the Wollastonite-Diopside subunit. Explanation

developed, given the P,T conditions appropriate to metamorphism of the Ethiudna Sub-block. If the formation of wollastonite according to reaction (1) had occurred in an essentially closed system, the nature of the reaction (ie. pure decarbonation), combined with the absence of coeval dehydration reactions, and the limited porosity under metamorphic conditions, would result in the reaction being buffered along the univariant curve(s) in Fig. 4. Since peak temperatures and pressures were less than 650°C and 4kbars, the reaction would cease after a relatively small degree of progress. Textural evidence from the Wollastonite-Diopside subunit, viz; high modal abundances of wollastonite and complete absence of the assemblages calcite-quartz and wollastonite-calcite-quartz, suggests that internal buffering did not occur. This implies that the  $X_{CO_2}$  of fluids during the petrogenesis of the Wollastonite Stage were constrained to values of less than ~0.18. Such a constraint necessitates an open system where  $CO_2$  is removed almost as fast as it is produced. Loss of  $CO_2$  via simple grain boundary diffusion is implausible given the likely rates of the  $CO_2$  production via reaction (1) (Rice & Baker, 1982). Thus the only geologically reasonable mechanism is infiltration of externally derived  $H_2O$ -rich fluids.

The process of fluid infiltration necessarily requires that a rock permeability be developed during the infiltrational event. The observation that non-buffered wollastonite-bearing assemblages are pervasively developed throughout the Wollastonite-Diopside subunit suggests that infiltration and therefore permeability were also pervasive. In the absence of any observable structural features which may have acted to focus infiltrating fluids, reaction-enhanced permeability (Valley, 1986), is suggested as a likely mechanism by which pervasive infiltration could occur, and is consistent with the large negative volume change (~33%; Valley, 1986) associated with reaction (1).

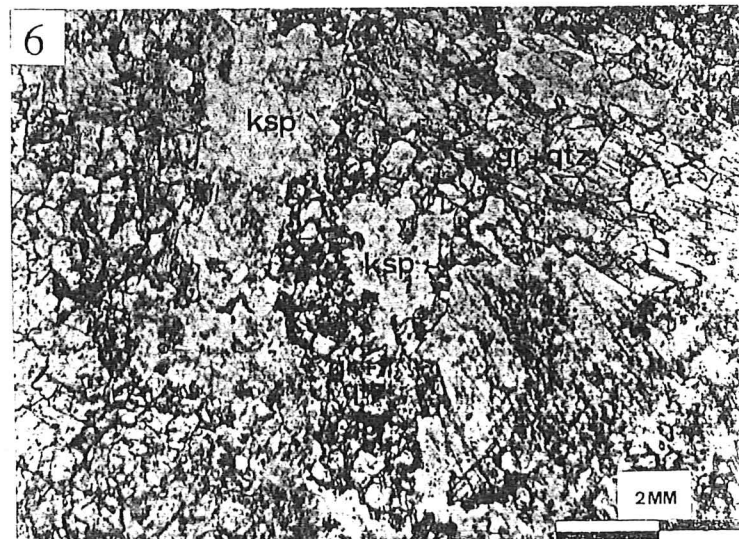
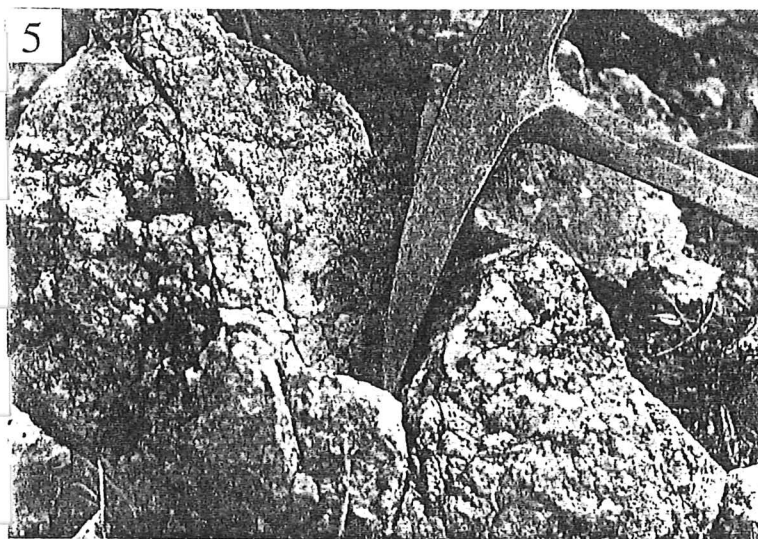
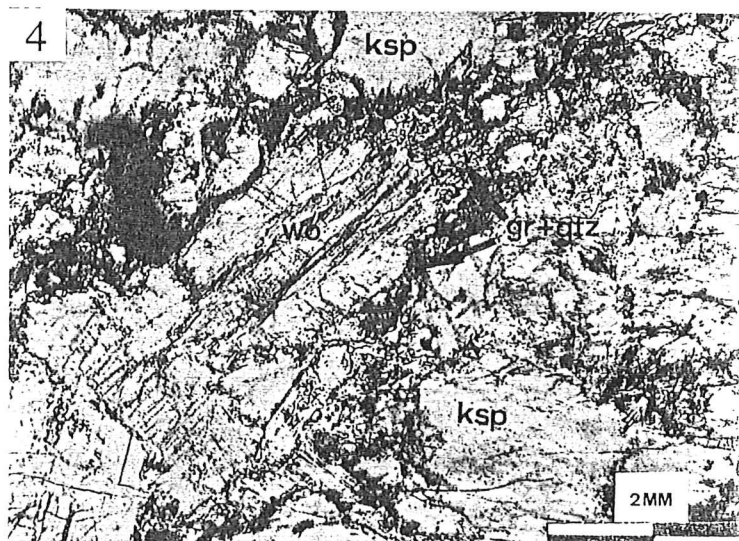
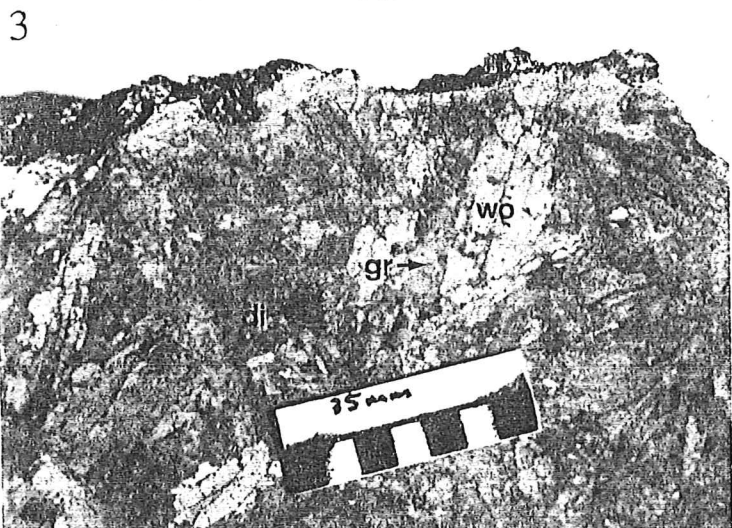
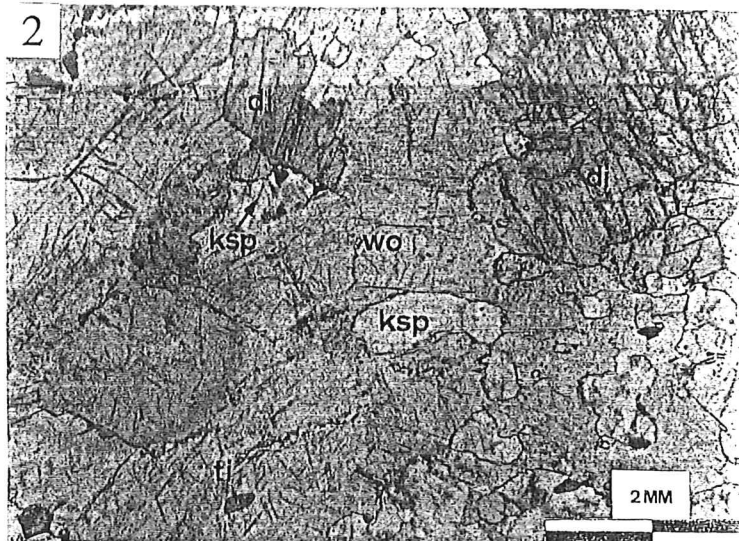
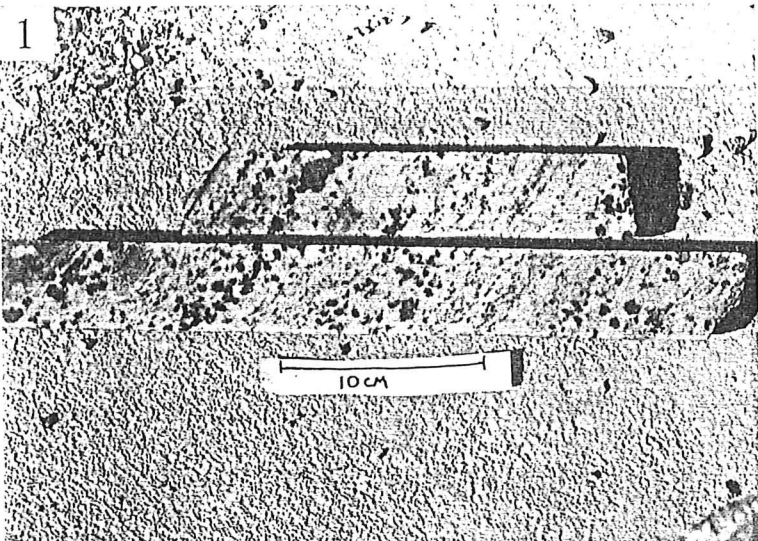
The textures which characterize the Grossular Stage suggest its formation in the Wollastonite-Diopside subunit is via the reaction;



The compositional changes involved in the reaction are a reflection of a decrease in the chemical potential ( $\mu$ ) of  $\text{K}_2\text{O}$  in the assemblage. This could conceivably occur due to changes in the P,T conditions during retrograde metamorphism of the wollastonite-microcline assemblage. However, the simple notion of a change in P,T conditions resulting in the initiation of reaction (2) is inconsistent with the large variations in reaction progress observed on outcrop scale (Plates 1 to 6), where a significant P,T differential is unlikely.

Such variations are more easily explained if it is assumed that the necessary changes in  $\mu\text{K}_2\text{O}$  accompany fluid infiltration-induced metasomatic depletion of  $\text{K}_2\text{O}$  from the wollastonite-microcline assemblage, and can be qualitatively represented by the use of a  $\mu\text{K}_2\text{O}$ - $\mu\text{CO}_2$  diagram. Fig. 5 is an isobaric, isothermal  $\mu\text{K}_2\text{O}$ - $\mu\text{CO}_2$  diagram for the system KCASH ( $\text{K}_2\text{O}$ - $\text{CaO}$ - $\text{Al}_2\text{O}_3$ - $\text{SiO}_2$ - $\text{H}_2\text{O}$ ) relevant to the reactions of interest in the Wollastonite-Diopside subunit. The slopes of univariant reaction lines are determined by the stoichiometric coefficients of  $\text{K}_2\text{O}$  and  $\text{CO}_2$  in the reactions, and the diagram is constructed using Schreinemaker's principles. The phase compositions, reactions and slopes are given in Appendix 7. The initial Wollastonite-Stage microcline-wollastonite-bearing assemblages are located in the stability field of both minerals in  $\mu\text{K}_2\text{O}$ - $\mu\text{CO}_2$  space (point (1)). A decrease in the  $\mu\text{K}_2\text{O}$  of the system induced by metasomatic removal of  $\text{K}_2\text{O}$  will result in the transposition of the assemblage across the univariant line for reaction (2) into the stability field of the grossular-quartz assemblage (point (2)). Variable degrees of metasomatic  $\text{K}_2\text{O}$  depletion due to varying fluid/rock ratios (F/R), would be reflected in corresponding variations in the progress of reaction (2), as observed.

Thus it seems probable on the grounds of textural evidence that the Grossular Stage assemblage was produced via a second episode of fluid infiltration. Furthermore, the localized distribution of this assemblage in the Wollastonite-Diopside subunit was controlled by; a) the





distribution of microcline-wollastonite-bearing assemblages, and b) the metasomatic fluid/rock ratios. Variations in fluid/rock ratios imply heterogeneous or focussed fluid flow, which can occur due to preferential movement of fluids along structurally-induced zones of high permeability. That structural features may have controlled the flow of metasomatic fluids associated with the Grossular Stage in the study area is suggested by the development of a relatively pure grossular-quartz rock in the Wollastonite-Diopside subunit (implying ~100% reaction progress), in a fold hinge at the Ethiudna East prospect. This hinge is a favourable dilational zone through which fluids could be channelled because of the competency difference between the Wollastonite-Diopside subunit and the overlying Calc-Silicate Quartzite. Thus high fluid fluxes localized to this zone resulted in greater reaction progress.

#### 3.4. AQUEOUS ELECTROLYTE COMPOSITIONS OF METASOMATIC FLUIDS

The composition and concentration of aqueous electrolytes in metamorphic fluids can have important implications for mineralization processes associated with infiltrational metasomatism. In order to evaluate the mineralizing potential of metasomatic fluids associated with the petrogenesis of the Bimba Suite, two techniques were implemented to characterize their aqueous electrolyte compositions; fluid inclusion analysis and scapolite analysis, the principles and results of which are described below.

##### 3.4.1. Fluid inclusion analysis

Microthermometric measurements performed on fluid inclusions in metamorphic minerals can be used to infer the compositions of metamorphic fluids, since the inclusions essentially constitute trapped samples of the fluids themselves. Furthermore, measurements of temperatures at which the contents of such inclusions homogenize can directly indicate the temperatures at which entrapment occurred during the growth of the host phase and thus characterize metamorphic temperatures.

With the aim of characterizing both metamorphic fluid compositions and temperatures, 16 such measurements were made on silicate minerals from the Bimba Suite. The sample group comprised Grossular Stage grossular from the Wollastonite-Diopside subunit, diopside from the Calc-Silicate Quartzite, and a Brittle-Fracture Stage quartz vein crosscutting the Calc-Silicate Quartzite at the Ethjudna East Prospect. Details of the implementation of microthermometric measurements are given, together with a tabulation of results, in Appendix 5.

Histograms showing temperatures of first melting ( $T_m$ ), final melting ( $T_{fm}$ ) and homogenization ( $T_{hom}$ ) of the inclusions are given in Fig. 6. The distinction between primary and secondary inclusions (ie. those trapped during, and subsequent to crystallization of the host mineral respectively) was made using criteria listed in Craig and Vaughan (1981), and estimates of fluid salinities were made using temperature-composition diagrams for the systems NaCl-H<sub>2</sub>O and CaCl<sub>2</sub>-H<sub>2</sub>O given in Crawford (1981a).

Grossular: Primary fluid inclusions in grossular displayed great variation in shape and morphology, with measurements being carried out on six inclusions ranging in size from 12 to 24  $\mu\text{m}$ . Both primary and secondary inclusions were simple two-phase (liquid + vapour) types with no daughter salts observed at room temperatures. Acicular aggregates typical of the habit of antarcticite (CaCl<sub>2</sub>.6H<sub>2</sub>O) were frequently observed to crystallize, however, during cooling of the inclusions below 0°C. The presence of CaCl<sub>2</sub> in the inclusions is further evidenced by the extremely low first melt temperatures of the fluid phase (Fig. 6). A CaCl<sub>2</sub>-dominated brine mixture, probably with MgCl<sub>2</sub>, NaCl and other species is proposed for the composition of the fluid phase rather than a pure CaCl<sub>2</sub> brine, since  $T_m$  values (-65°C to -70°C) are well below the -49.8°C eutectic for the CaCl<sub>2</sub>-H<sub>2</sub>O system (Crawford, 1981a).  $T_{fm}$  values ranging from -26° to -32°C correspond to salinities of 11 to 13 wt.% CaCl<sub>2</sub> equivalent. No visual or microthermometric evidence of CO<sub>2</sub> was found, which is consistent with the observation that

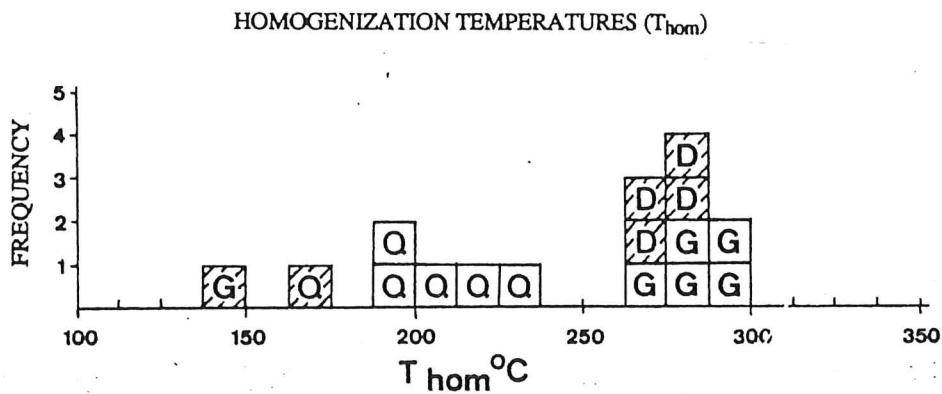
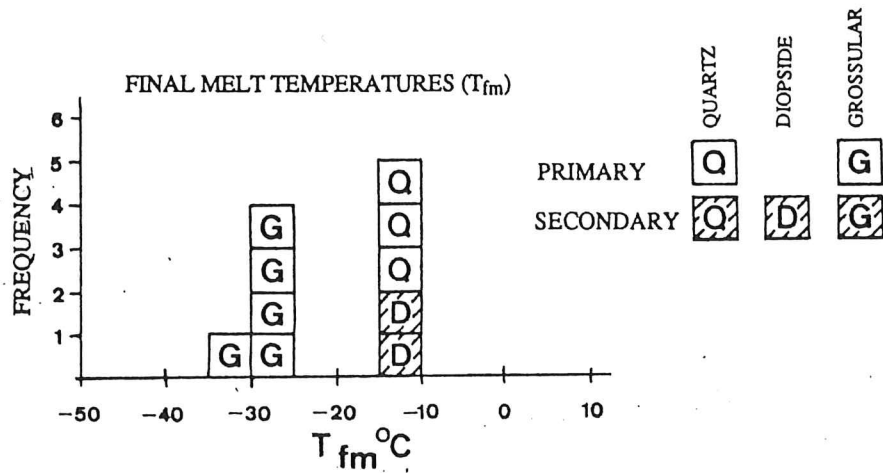
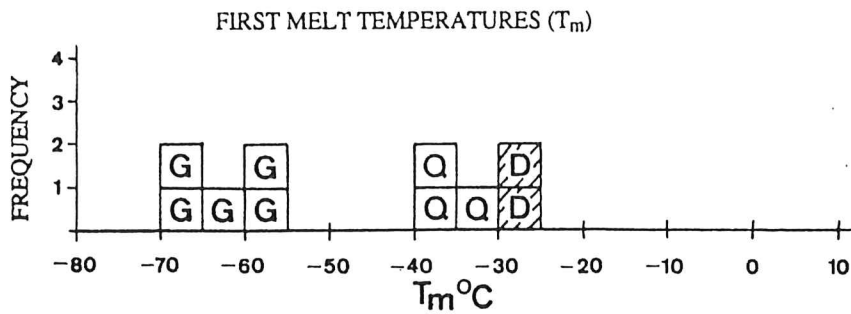


FIGURE (6): Histograms of data for first melt, final melt, and total homogenization temperatures of grossular, diopside, and quartz fluid inclusions.

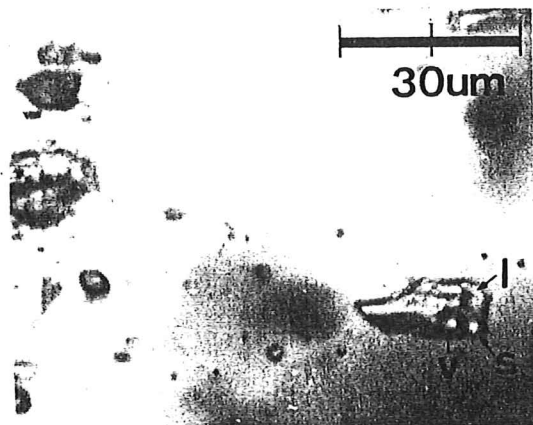


PLATE (7): Secondary, three phase (l+v+s) inclusion in diopside, showing cubic daughter salt (halite).

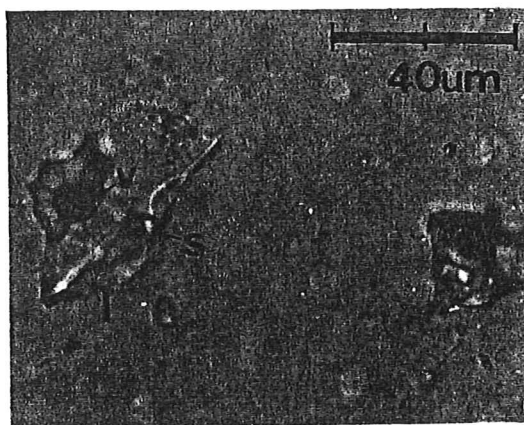


PLATE (8): Primary, three phase (l+v+s) inclusions in Brittle-Fracture Stage quartz with large, euhedral, halite daughter salts.



of primary inclusions ranged from 260° to 298°C, suggesting the formation of the Grossular Stage took place during the later stages of retrograde metamorphism.

Diopside; All fluid inclusions observed in diopside grains were three-phase (+liquid+vapour+solid) with barely resolvable cubic daughter salts (Plate 7). The inclusions are secondary, as indicated by their  $T_{\text{hom}}$  (266° to 280°C), which imply temperatures too low for diopside crystallization, and by their occurrence aligned in planes which is suggestive of trapping during fracture healing. The similarity of  $T_{\text{hom}}$  of these inclusions and those of primary grossular inclusions suggests this fracture healing may have occurred during fluid infiltration associated with the Grossular Stage. Considerable disparity exists between the brine compositions of grossular and diopside inclusion fluids, however.  $T_{\text{m}}$  values (-27.4°C) are close to the metastable NaCl-H<sub>2</sub>O eutectic (-28°C; Crawford, 1981a) implying that the fluids are essentially pure NaCl brines. Melting at the metastable eutectic can be explained by the high heating rates used during microthermometric measurements (0.5-1°C/second).  $T_{\text{fm}}$  values suggest fluid salinities of 16 to 17 wt.% NaCl equivalent.

Quartz; Primary fluid inclusions in Brittle-Fracture Stage quartz are large (up to 40µm), three-phase types (ie. liquid + vapour + solid; Plate 8). The inclusion fluids are proposed as being NaCl-rich (as suggested by the presence of cubic daughter salts) with admixtures of other species such as CaCl<sub>2</sub> or MgCl<sub>2</sub>, the presence of which has resulted in the depression of  $T_{\text{m}}$  values (-34° to -35°C) below the NaCl-H<sub>2</sub>O eutectic.  $T_{\text{fm}}$  values are in the range -12.3° to -13.4°C implying salinities of 16-17 wt% NaCl equivalent. Temperatures from 179 to 240°C are suggested for the formation of Brittle-Fracture Stage quartz veins, on the basis of the  $T_{\text{hom}}$  of the five primary inclusions examined.

#### 3.4.2. Scapolite analysis

Solid solution in scapolite involving marialite (Na<sub>4</sub>Al<sub>3</sub>Si<sub>9</sub>O<sub>24</sub>Cl), and meionite (Ca<sub>4</sub>Al<sub>6</sub>Si<sub>6</sub>O<sub>24</sub>CO<sub>3</sub>), has been implicated as a potential sensor of fluid salinity in metamorphic

environments (Orville, 1975; Ellis, 1978; Vanko & Bishop, 1980). The NaCl content of scapolites, ie. the proportion of the marialite end member, is controlled (in the presence of calcite) by the exchange equilibrium:



Ellis (1978), calculated  $K_D$ 's for the exchange at 750°C and 4kbars via analysis of scapolites synthesized in equilibrium with fluids of known NaCl/(NaCl + H<sub>2</sub>O) ratios, and derived the relation:  $\ln K_D = -0.0028(X_{Al})^{-5.5580}$  where  $X_{Al} = \text{Al}/(\text{Al} + \text{Si})$  in scapolite. This relation can be used to calculate the salinity of fluids in equilibrium with scapolite of known Cl/(Cl + CO<sub>3</sub>) ratios at 750°C and 4kbars. The correlation between scapolite composition and fluid composition at these P,T conditions is shown in Figure 8. The utility of this method of fluid composition characterization is that the NaCl-CO<sub>3</sub> composition of scapolites only reflects the composition of fluids present during the crystallization of the mineral. Once crystallized, scapolites are remarkably impervious to compositional alteration via exchange of Cl and CO<sub>3</sub> with inequillibrated fluids, as experimentally demonstrated by Ellis (1978). This behavior is a consequence of Cl and CO<sub>3</sub> anions being trapped in cage-like structures formed by Al-Si tetrahedra during crystal growth (Levien & Papike, 1976).

Thirty scapolites from the study area were analysed using the wavelength dispersive system on a JEOL 733 Microanalyser. The sample group comprised 12 analyses from calcite-poor layers of the Calc-Silicate Quartzite, including 6 from a scapolite pod, and 18 analyses from calcite-rich zones of the subunit at the Ethudna East Prospect. Scapolite formulae were calculated based on Al+Si=12, and CO<sub>3</sub> contents, which could not be determined by microprobe analyses, were calculated using the assumption that Cl+SO<sub>4</sub>+CO<sub>3</sub>=1. Scapolite compositions are expressed in terms of their equivalent anorthite content (EqAn), where  $\text{EqAn} = 100(\text{Al}-3)/3$  (Fig. 7).

The results of these analyses (tabulated in Appendix 3) are superimposed on Fig. 8, and can be seen to define two populations which separate scapolites from calcite-poor layers and scapolites from calcite-rich zones of the subunit. Although the absolute figures for salinity of coexisting fluids shown on the diagram will vary for P,T conditions other than those specified, they are suggested as being a reasonable approximation for amphibolite-facies conditions (Oliver et al., 1992).

More importantly however, are the implications for the differing salinity of fluids in equilibrium with scapolites from the same subunit. Two scenarios are outlined below which could account for the observed differences. In the first, internal buffering of fluids within layers of variable primary evaporitic content could have resulted in the crystallization of less Cl-rich scapolites in the more siliceous layers, the implication being that such layers had lower primary NaCl contents relative to the carbonate-rich layers. That such within-layer buffering can result in marked differences in NaCl-contents of scapolites on a hand-specimen scale has been convincingly demonstrated by Oliver et al.(1990).

In the second scenario, external buffering via a saline fluid infiltration could have occurred, with the differences in NaCl-content of scapolites reflecting variation in fluid/rock ratios. Higher fluid/rock ratios would be expected for the more carbonate-rich layers owing to the more extensive development of reaction-enhanced permeability implied by the greater modal abundance of calc-silicates in these layers. Thus lower input of NaCl-bearing fluids in carbonate-poor zones would be reflected in the lower NaCl contents of scapolites crystallized therein.

The latter scenario is suggested as more likely as it is consistent with the conclusion made earlier that fluid infiltration occurred during Bimba Suite petrogenesis. The close spatial relationship between carbonate-rich zones of the Calc-Silicate Quartzite and the Wollastonite-Diopside subunit suggest they were probably infiltrated by the same fluids during

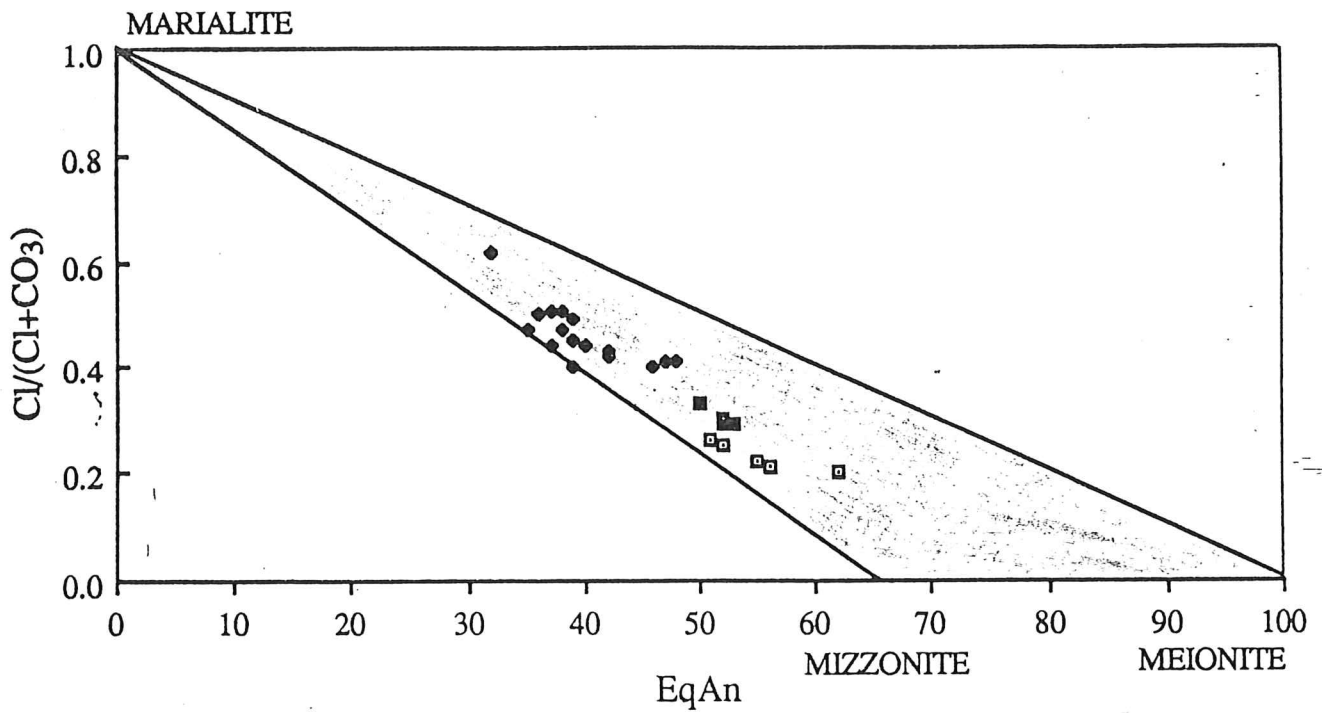


FIGURE (7): Compositions of scapolites from the Calc-Silicate Quartzite, shown within the stability field of natural scapolites (shaded area; after Ellis, 1978).

- Scapolites from calcite-poor layers
- ◆ Scapolites from calcite-rich layers
- Scapolites from scapolite pod

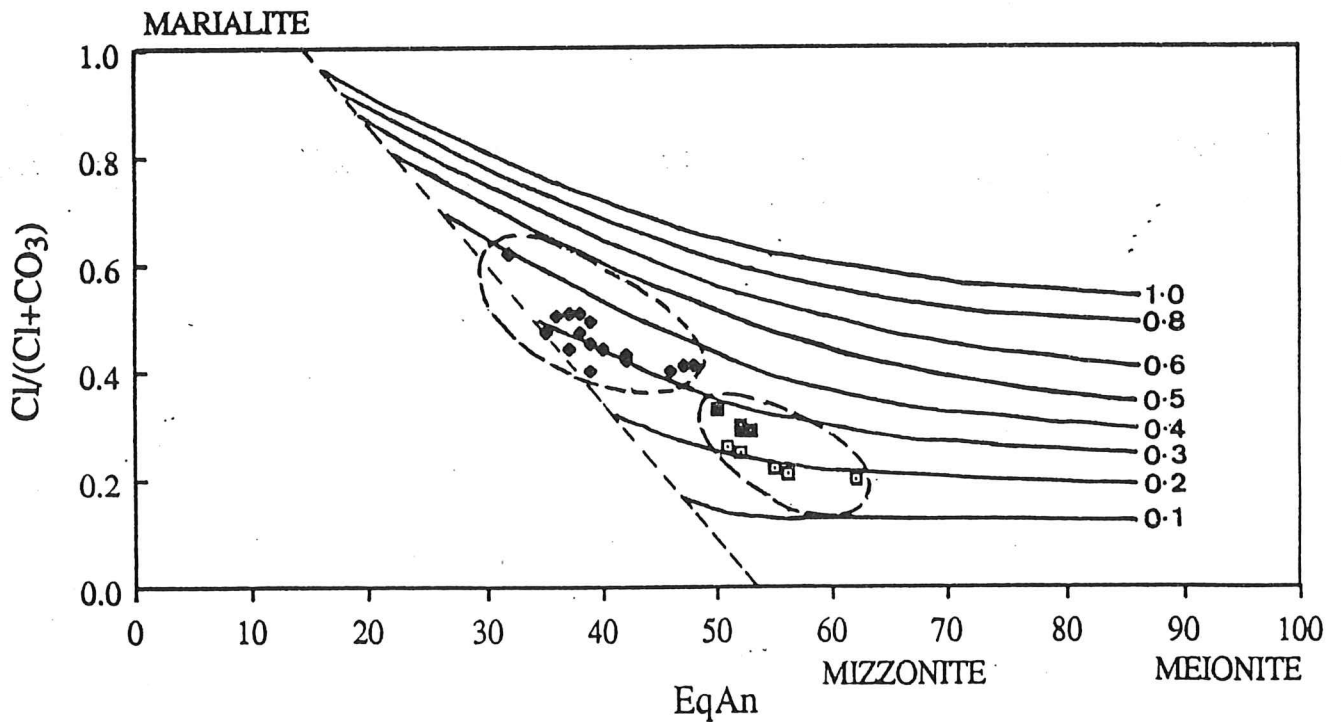


FIGURE (8): Correlation between scapolite composition and fluid composition. Lines of equal  $\text{NaCl}/(\text{NaCl}+\text{H}_2\text{O})$  in coexisting fluid at 750°C and 4kbars are shown (after Ellis, 1978), together with the compositions of Ethudna scapolites.

metamorphism. Crystallization of scapolites is suggested as occurring coevally with the formation of Wollastonite Stage assemblages. This suggestion is based on the observation of textural equilibrium between scapolites and phases of the Wollastonite Stage assemblages, which are locally developed in the Calc-Silicate Quartzite. Thus it seems probable in the light of the known metamorphic P,T history of the Bimba Suite that the formation of both phases took place during fluid infiltration during prograde heating, and that therefore the salinities of infiltrating fluids, as inferred from scapolite compositions, are also representative of those involved in the development of the Wollastonite-Stage assemblages. Growth of the scapolites during the Grossular Stage is precluded on the basis of;

- a) temperatures inferred for the formation of the Grossular Stage based on fluid inclusion data are below that of the stability field of scapolites, and
- b) the extremely low  $X_{CO_2}$  of Grossular Stage fluids as inferred from fluid inclusion data are unfavourable for the growth of scapolite (Ellis, 1978).

#### 3.4.3. Origin of high metamorphic fluid salinities

The relatively high salinities of fluids associated with both prograde and retrograde metamorphism of the Bimba Suite as inferred from petrological data above, are consistent with conclusions made by Cook and Ashley (1992) that the unit represents a meta-evaporite/carbonate sequence. Saline fluid inclusions, frequently containing  $CaCl_2$ , and scapolites with high NaCl contents are characteristic of such sequences which have been metamorphosed to amphibolite facies (Crawford, 1981b; Oliver et al., 1990).

### 3.5 CARBON-OXYGEN STABLE ISOTOPE GEOCHEMISTRY OF THE BIMBA SUITE

The stable oxygen isotopic signatures of marbles embedded in silicate sequences have been used extensively to provide insight into the extent of fluid-rock interaction during metamorphism, because of the step function defined by the large initial difference in the oxygen isotope composition between the two lithologies ( $\approx 10\%$ ). Techniques which involve the construction of an oxygen isotope profile across such marble beds have been used to quantify the advective flux of fluids in region metamorphic terrains (Bickle & McKenzie, 1987; Bickle & Baker, 1990). The application of such techniques to this study was undertaken with the aim of quantifying fluid advection, which has been demonstrated, via petrological evidence, to have occurred during the petrogenesis of the Wollastonite-Diopside subunit.

Samples for two isotopic profiles, measuring 2.10 and 0.49 metres respectively, were extracted from drill-core, which had intersected two marble beds in the Wollastonite-Diopside subunit at the Ethiudna East prospect. No marble layers of comparable thickness were intersected by drilling at the Ethiudna mines, however samples from the same subunit were taken from thin (<20cm) marble layers associated with sulphides in drillcore, and from blocks of marble up to 30cms across present in the spoil heaps of the Main Shaft at the locality. Since facilities for the isotopic analysis of silicates were not available, their  $\delta^{18}\text{O}$  was measured indirectly, via the analysis of small (<0.5cm), isolated, calcite grains imbedded in silicate phases. This was done with the assumption that the small size of the grains would allow diffusional processes to isotopically equilibrate the two phases, with the equilibrium  $\delta^{18}\text{O}$  of the calcite approaching that of the more voluminous silicate phase. Five such measurements were taken of calcite associated with wollastonite, diopside and grossular in the Wollastonite-Diopside subunit at the Ethiudna East prospect.

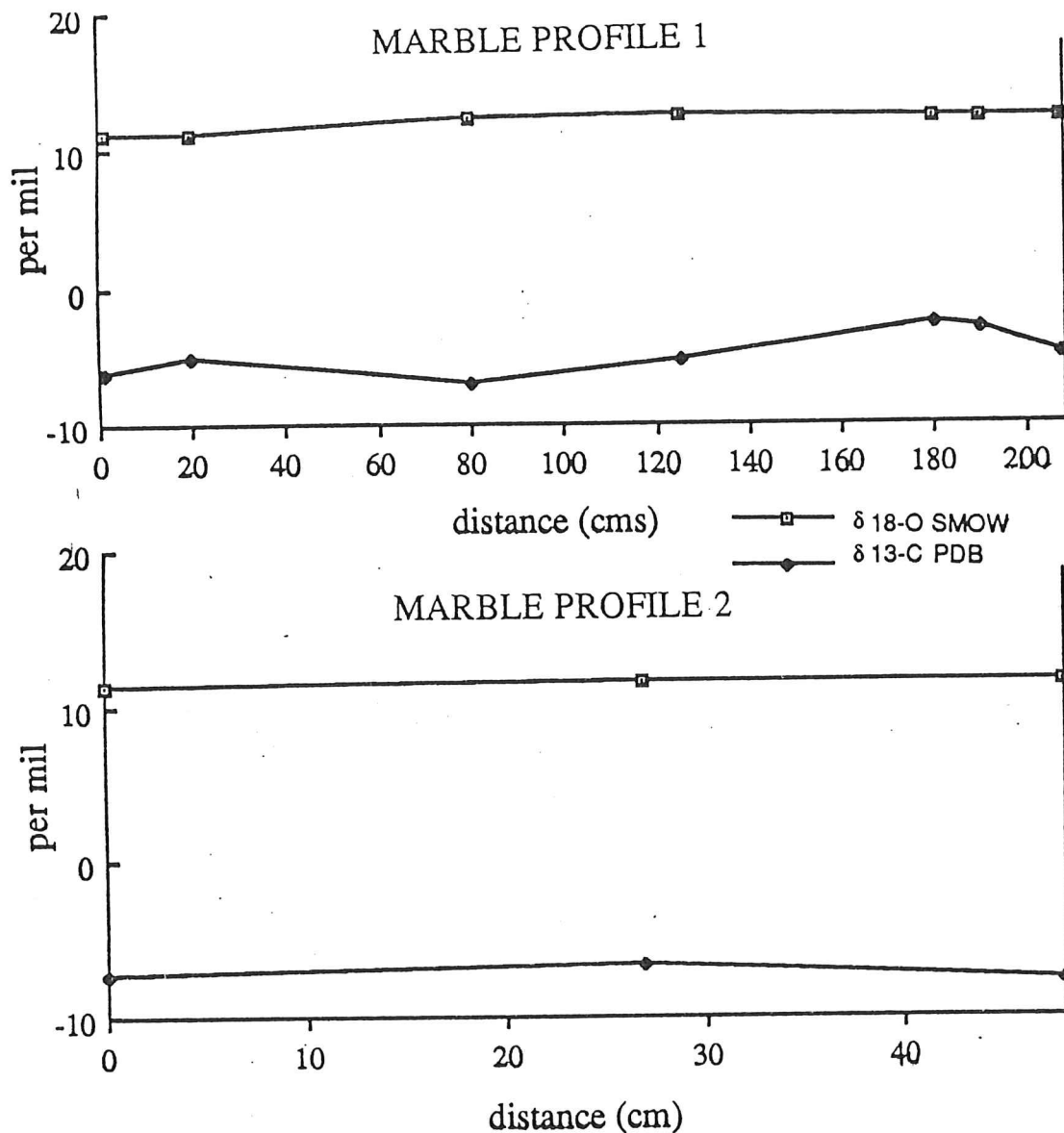


TABLE (3): CARBON-OXYGEN ISOTOPE ANALYSES OF ETHIUDNA CARBONATES

SAMPLE	SETTING	18-O	13-C
		SMOW	PDB
RW-1	calcite embedded in coarse wollastonite,EEC	13.1	-8.2
RW-2	calcite embedded in coarse wollastonite,EEC	12.9	-9.3
RW-3	calcite embedded in coarse wollastonite,EEC	13.0	-9.2
RW-4	calcite embedded in coarse wollastonite,EEC	11.4	-9.9
RW-5	calcite embedded in coarse wollastonite,EEC	11.4	-10.8
EMS-1	coarse marble from Main Shaft dumps	13.6	-2.9
EMS-2	coarse marble from Main Shaft dumps	13.5	-2.8
EMS-3	coarse marble from Main Shaft dumps	13.7	-2.7
EEC-1-A	marble profile 2, Ethiudna East Prospect	11.3	-7.3
EEC-1-B	marble profile 2, Ethiudna East Prospect	11.6	-6.6
EEC-1-C	marble profile 2, Ethiudna East Prospect	11.6	-7.6
EEC-2-I	marble profile 1, Ethiudna East Prospect	11.1	-6.2
EEC-2-II	marble profile 1, Ethiudna East Prospect	11.2	-5.1
EEC-2-III	marble profile 1, Ethiudna East Prospect	12.3	-7.0
EEC-2-IV	marble profile 1, Ethiudna East Prospect	12.5	-5.4
EEC-2-V	marble profile 1, Ethiudna East Prospect	12.4	-2.6
EEC-2-VI	marble profile 1, Ethiudna East Prospect	12.4	-3.0
EEC-2-VII	marble profile 1, Ethiudna East Prospect	12.4	-5.0
CMS-1	marble with sulphides, Ethiudna mines	12.3	-9.2
CMS-2	marble with sulphides, Ethiudna mines	12.4	-9.2



The results for all C-O analyses are quoted in  $\delta^{18}\text{O}_{\text{SMOW}}$  and  $\delta^{13}\text{C}_{\text{PDB}}$  and are listed in Table 3.  $\delta^{18}\text{O}$  values of all samples analysed are highly uniform (range 11.1-13.7‰) and the two marble profiles (Fig. 9) indicate that complete isotopic homogenization has occurred between the marbles and the enclosing wollastonite-dominated calc-silicate rocks. The  $\delta^{18}\text{O}$  values of the marbles are a substantial departure from the primary isotopic signature of their presumed precursor Proterozoic limestones which typically fall within the range 23-35‰ (Taylor, 1979).

The modifications to the primary signatures of carbonates during metamorphism may result from one or more of the following processes;

1/ devolatilization reactions

2/ diffusion of isotopes between the carbonate bed and adjacent lithologies

3/ isotopic exchange with infiltrating fluids

Devolatilization reactions such as reaction (1), may result in  $^{18}\text{O}$  and  $^{13}\text{C}$  depletions due to preferential partitioning of the heavier isotopes into the evolved  $\text{CO}_2$ . Devolatilization alone cannot account for the inferred isotopic shift of the marbles owing to the restrictions placed on decarbonation reactions by their purity. Substantial shifts may have occurred during the formation of the wollastonite rocks adjacent to the marble beds where the high modal abundance of wollastonite infers substantial loss of  $\text{CO}_2$  via decarbonation. However even assuming total decarbonation, maximum predicted isotopic shifts are in the order of 6-7‰ (Valley, 1986) which fall short of the inferred shift of 10-22‰.

The timescales over which diffusion alone could act to completely homogenize the marble bed can be calculated by applying the equation derived by Bickle and McKenzie (1987) for chemical diffusion in the presence of a fluid phase;



$$t = \frac{h^2}{D_{\text{eff}}} \left( \frac{\rho_s}{\rho_f} + \phi \right) t' \quad (5)$$

where  $t$  is time (seconds),  $h$  is the thickness of the solid phase (metres),  $D_{\text{eff}}$  is the effective diffusivity of the two phase material,  $\rho_s$  is the solid density (gm/cc),  $\rho_f$  is the fluid density (gm/cc),  $K_c$  is the distribution coefficient between fluid and solid,  $\phi$  is the porosity, and  $t'$  is a dimensionless time constant. For the case of the larger marble profile;  $h = 2.10$  m;  $D_{\text{eff}} = 10^{-11}$ ;  $\rho_s = 2.8$  gm/cc;  $\rho_f = 1$  gm/cc;  $K_c = 1.8$ ; and  $\phi = 10^{-3}$ . The geometry of the profile is essentially identical to theoretically-derived profiles for pure diffusion given a  $t'$  of 0.4 (Bickle & McKenzie, 1987). Substitution of these values into equation (5) gives a minimum time requires for total isotopic homogenization of approximately 30,000 years, assuming a realistic porosity of  $10^{-3}$ . Given the timescales involved in metamorphic processes it seems possible that isotopic homogenization of the marble bed could have occurred via diffusion alone. This does not however, preclude the possibility of homogenization as a result of fluid infiltration, and indeed the high degree of isotopic homogeneity of both silicate and carbonates throughout the Wollastonite-Diopside subunit together with the fact that the isotopic shifts inferred for the calc-silicates cannot be explained by devolatilization alone, is a strong argument for the involvement of the process. If infiltration is assumed, isotopic exchange between the externally derived fluids equilibrated with a siliciclastic sequence (eg. the Quartzofeldspathic Suite), and the calc-silicates and carbonates of the Bimba Suite provides a plausible explanation for the large isotopic shifts inferred for the latter unit, especially when the high efficiency of the infiltration process relative to diffusion is taken into consideration.

## CHAPTER 4 : SULPHIDE PETROLOGY AND GENESIS

### 4.1. THE NATURE AND DISTRIBUTION OF PRIMARY SULPHIDE MINERALIZATION

Primary sulphide mineralization, from which all the secondary Cu-Co mineralization in the Ethiudna area was ultimately derived, forms a significant, albeit subeconomic, component of the Bimba Suite and Quartzofeldspathic Suite metasediments. A study of the mineralogy, petrology and distribution of this mineralization, represented by eight sulfide and one arsenide species (Table 4), was undertaken in order to define the nature and relative timing of the mineralizing event(s) and its relationship to the metamorphic processes previously described.

With few exceptions, unaltered primary mineralization is rare in outcropping metasediments of the Ethiudna area, thus sulphide sampling for the most part, was limited to drill core. Detailed observation and sampling of some 1.5km of drill core, from both the Ethiudna mines and the Ethiudna East prospect, has enabled the stratigraphic and spatial distribution of sulphides to be accurately determined (Fig. 10).

#### 4.1.1. Ethiudna mines

The bulk of the sulphide mineralization at the Ethiudna mines is present in the microclinolites of the Quartzofeldspathic Suite. These sulphides consisting predominantly of cobaltian pyrite with lesser chalcopyrite and pyrrhotite are present as;

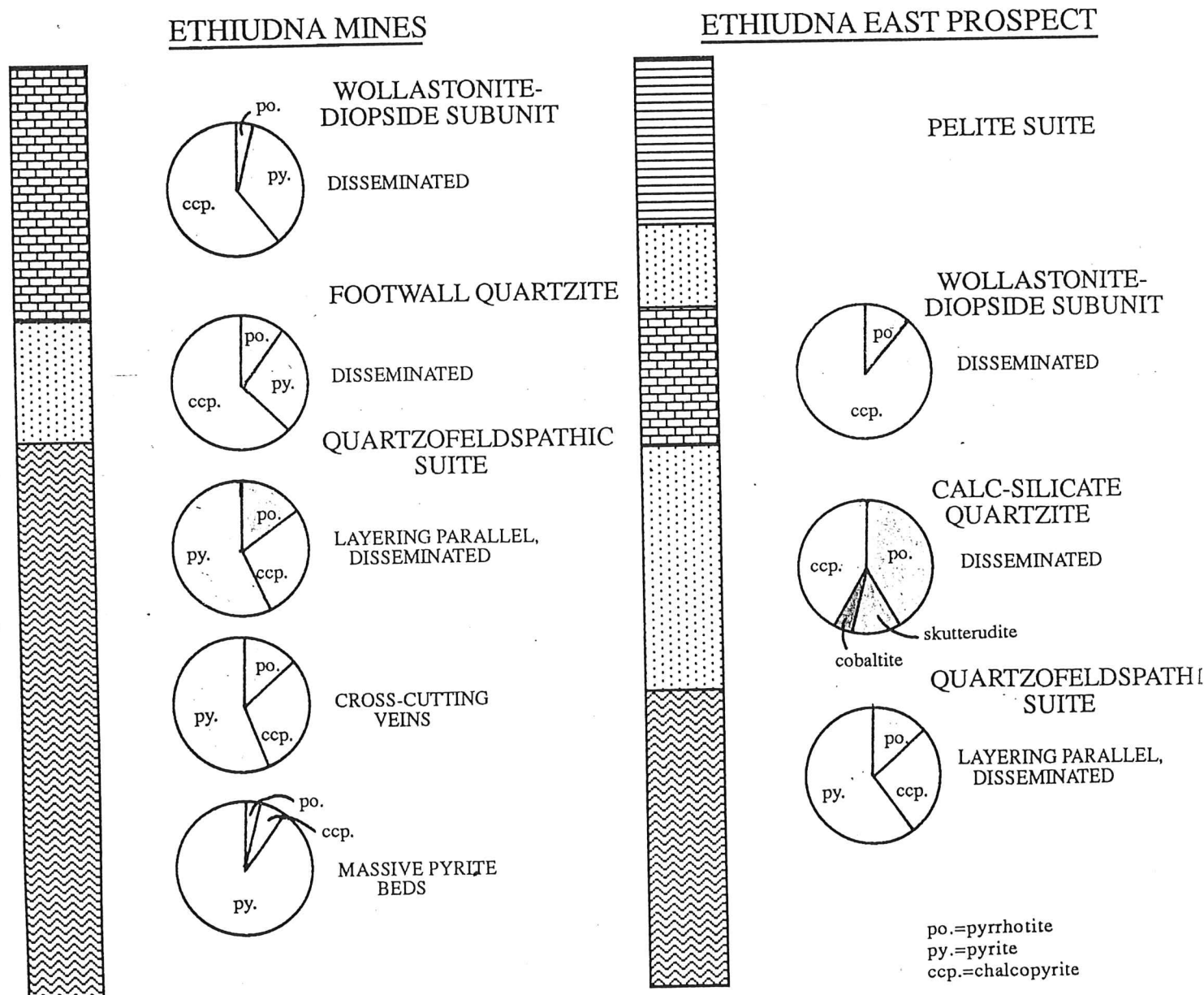
- a) mono- and polyminerallic disseminations,
- b) thin (2-10mm) polyminerallic layers oriented parallel to microclinolite  
compositional layering,
- c) rare, thin (2-10mm) polyminerallic veins crosscutting microclinolite layering

TABLE (4): MINERALOGY OF SULPHIDE MINERALIZATION

MINERAL	PARAGENETIC POSITION	ABUNDANCE ETH. MINES	ABUNDANCE ETH. E. PROS.	FORM	COMPOSITIONAL VARIATION
bornite	P	r	u	a	Cu <sub>4.52-4.91</sub> Fe <sub>0.98-1.08</sub> Co <sub>0.01-0.04</sub> S <sub>4.09-4.14</sub>
chalcocite	S	u	-	a	Cu <sub>1.91-1.94</sub> S <sub>1.05-1.07</sub>
chalcopyrite	P	c	c	a,e	Cu <sub>0.99-1.03</sub> Fe <sub>0.96-1.02</sub> S <sub>2.00-2.03</sub>
cobaltite	P	-	c	e	Co <sub>0.63-0.95</sub> Fe <sub>0.04-0.10</sub> Ni <sub>0.02-0.1</sub> As <sub>0.99-1.34</sub> S <sub>0.83-1.00</sub>
marcasite	S	u	c	a	not analysed
molybdenite	P	u	-	a,s	not analysed
pyrite, cobaltian	P,R	c	u	e,s	Fe <sub>0.85-1.01</sub> Co <sub>0-0.15</sub> S <sub>1.88-2.0</sub>
pyrrhotite	P	c	c	a,e	Fe <sub>0.84-.95</sub> Co <sub>0-0.01</sub> Ni <sub>0-0.01</sub> S <sub>1.05-1.16</sub>
skutterudite	P	c	a	a	Co <sub>0.97-0.98</sub> Ni <sub>0.01-0.02</sub> Fe <sub>0.03-0.04</sub> As <sub>2.95-2.96</sub>

P=pre or syn-peak metamorphism, R=retrograde metamorphic, S=supergene, c=common, u=uncommon, r=rare, -=not observed, a=anhedral, e=euhedral, s=subhedral.

FIGURE (10): SULPHIDE SPECIES PROPORTIONS; STRATIGRAPHIC VARIATION



d) rare, massive cobaltian pyrite beds up to 1 m thick.

Mineralization in the overlying Footwall Quartzite and Wollastonite-Diopside subunits of the Bimba Suite is dominated by chalcopyrite as disseminations with lesser cobaltian pyrite and pyrrhotite. Traces of both pyrite and chalcopyrite were noted in the leucosomes of migmatized microclinolite and in adamellite where it intruded sulphide-bearing microclinolite. Such sulphide occurrences presumably result from wallrock contamination of the adamellite, since no sulphides were observed in the intrusions at any significant distance from the microclinolite contact, nor in pegmatites or quartz veins associated with adamellite bodies.

#### 4.1.2. Ethiudna East prospect

Microclinolite-hosted mineralization at the Ethiudna East prospect is texturally and mineralogically identical to that observed at the Ethiudna mines. Mineralization in the overlying Bimba Suite is characterized by a more sulphur-deficient assemblage than that of the Ethiudna mines, and is dominated by pyrrhotite, chalcopyrite and lesser skutterudite and cobaltite, all of which are present as sparse disseminations.

#### 4.1.3. Other sulphide occurrences

Disseminated chalcopyrite, cobaltian pyrite and rare molybdenite were noted in the Wollastonite-Diopside subunit outcropping approximately 1km west of the Ethiudna East prospect. Observations of sulphide distributions elsewhere in the study area were hampered by lack of drill core, however the occurrence of layer-parallel gossans in outcropping microclinolites was widespread. These gossans are suggested as representing the oxidised equivalents of similarly occurring sulphide mineralization observed in drill core, a hypothesis supported by their anomalous Cu and Co content (up to 1.29 and 0.07% respectively), and the frequent development of conspicuous secondary copper mineralization (chrysocolla, tenorite) in graphitic metapelites proximal to the gossan-bearing microclinolites.

## 4.2. ORE TEXTURES AND MINERALOGY

Textures observed in Ethiudna sulphides and arsenides are typical of those present in ore bodies which have undergone regional metamorphism to amphibolite facies (Stanton, 1972; Lawrence, 1972; Mookherjee, 1976). Grain size is typically medium to coarse (0.2-5mm) and locally attains 15mm in remobilized pyrite. Evidence of textural equilibrium such as 120° triple-grain junctions in single phase aggregates, and arcuate boundaries between phases are abundant, indicating annealing recrystallization during metamorphism (Lawrence, 1972).

The mineral chemistry, associations and textural characteristics of each species observed at Ethiudna is described below. Microprobe analyses of sulphides are given in Appendix 4.

**PYRITE:** All pyrites analysed are cobaltian (Fig. 12), with cobalt contents ranging from 0.05 to 7.08% (mean 1.58%). Nickel contents are always correspondingly lower, and considerable variation in the Co:Ni ratios suggests no sympathetic relationship exists between the two elements. Pyrites also commonly contain low percentages of arsenic, and a weak correlation exists between arsenic and cobalt content. Such arsenic is probably present as an impurity within the pyrite lattice and/or as sub-microscopic inclusions of arsenide phases. Its presence accounts for the abundance of arsenates such as cornwallite and conichalcite in secondary ores of the Ethiudna mines, since visible arsenide phases have not been observed in the primary mineralization. Three genetic types of pyrite have been recognized;

(1) Large (1-4mm) euhedral to subhedral pyrite crystals (Plate 9), which predominate in microclinolite-hosted mineralization are interpreted as premetamorphic, on the basis of ; a) their lack of inclusions of surrounding sulphide phases, and b) the presence of prominent growth zoning defined by variation in cobalt content (Plate 17). Such zoning is common in hydrothermally deposited bravoites and cobaltian pyrites (Ramdohr, 1969; Springer et al.,



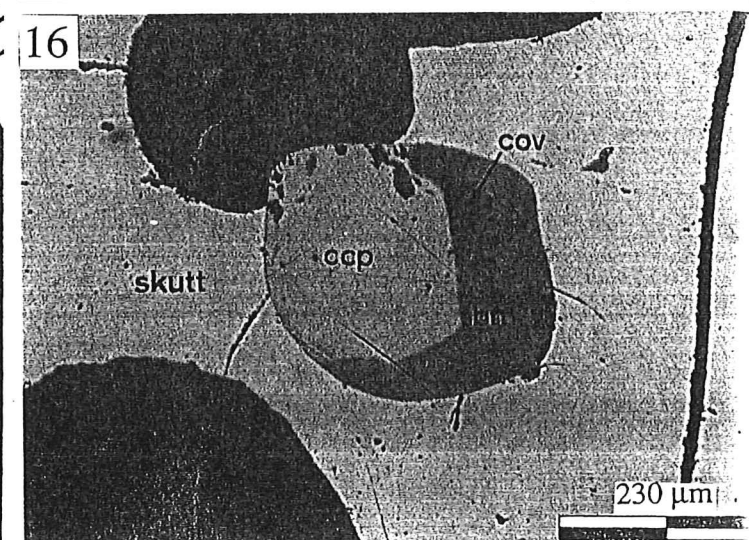
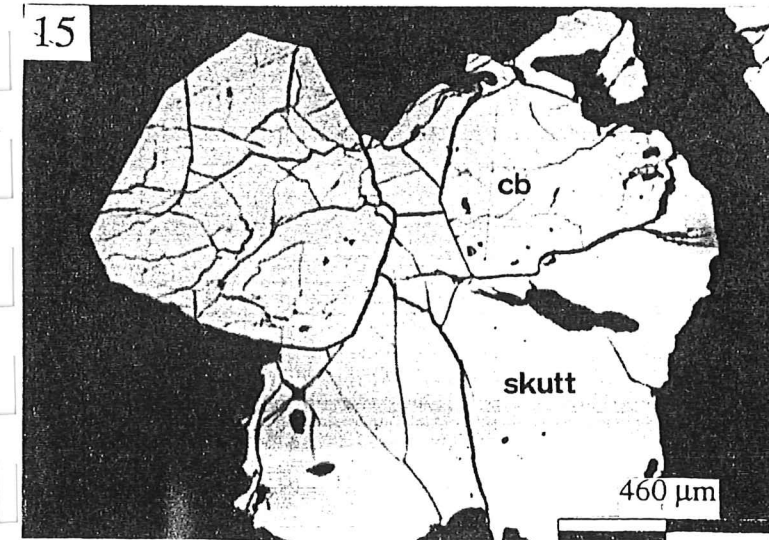
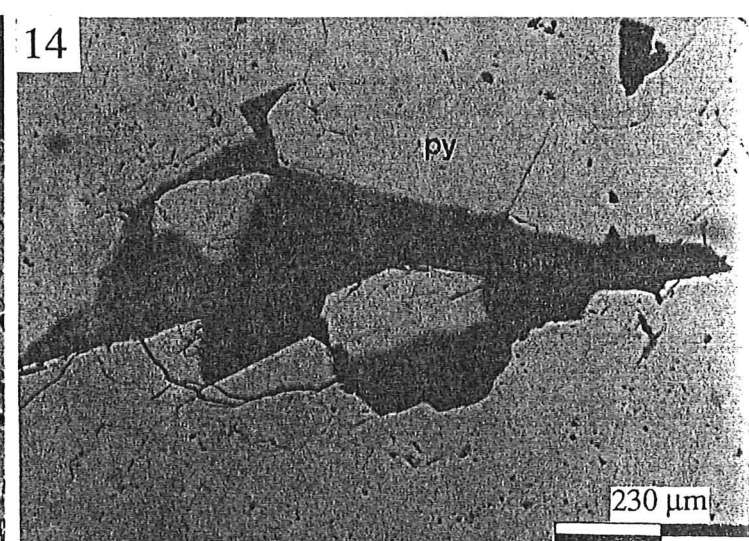
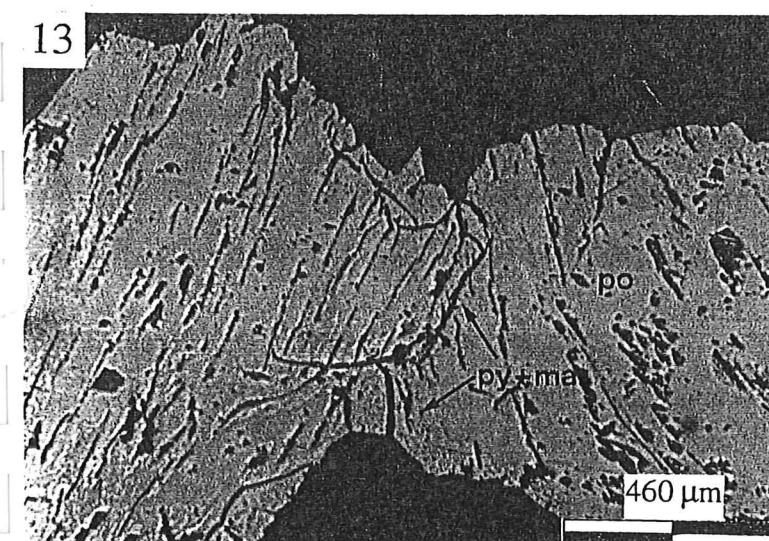
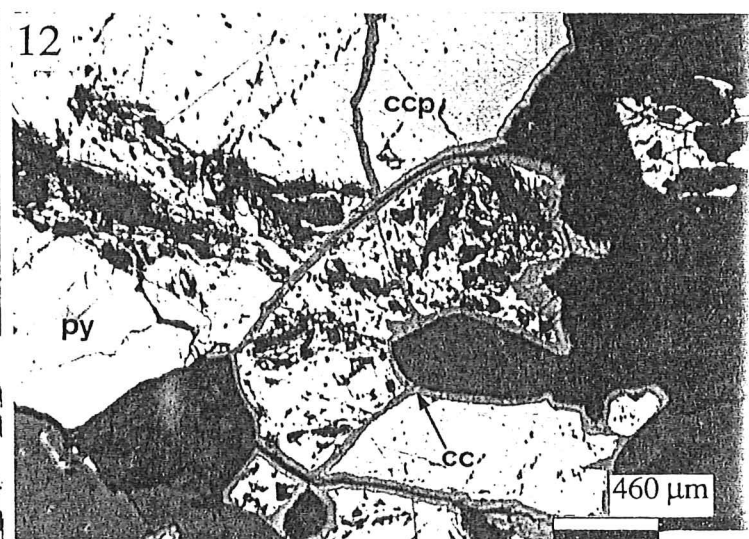
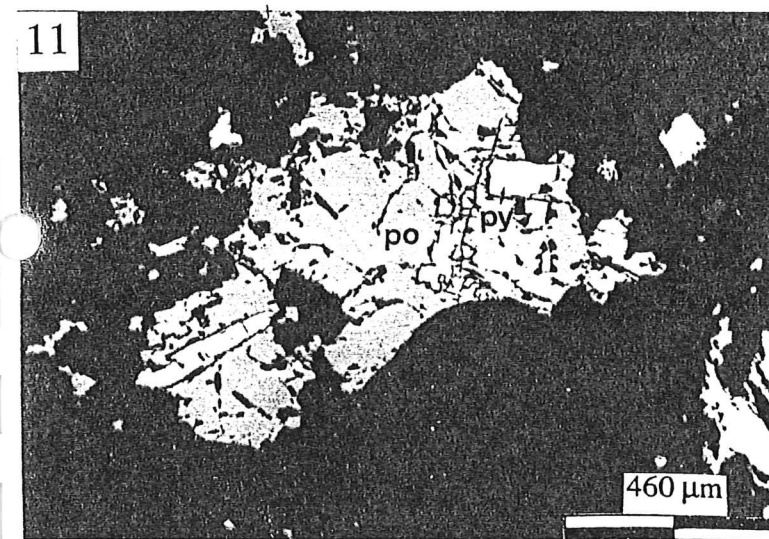
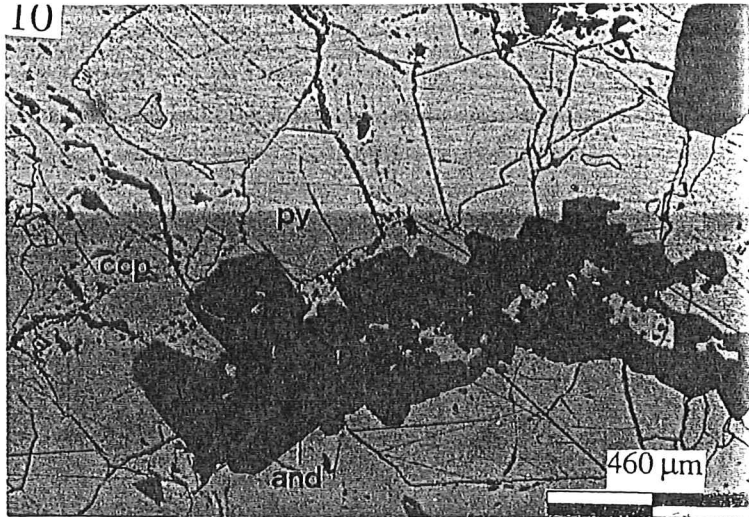
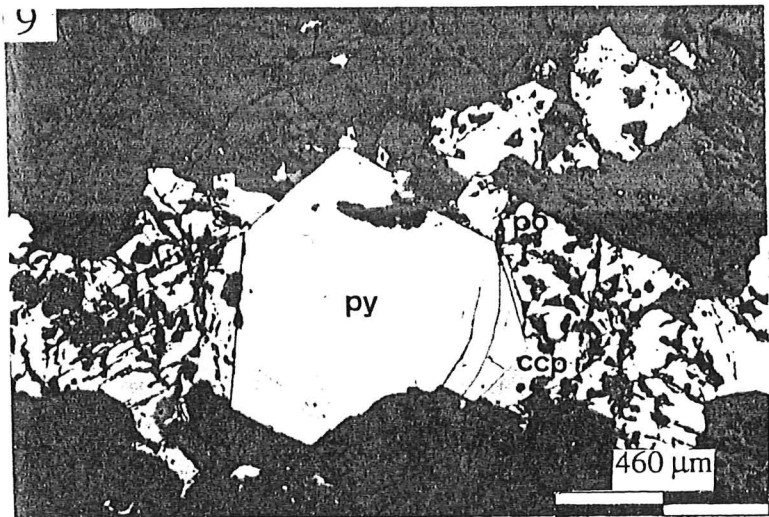


FIGURE (11): T-X diagram for phase relations in the system Fe-S (after Craig, 1990), showing narrowing stability field of pyrrhotite with decreasing temperature. Cooling path shown (dashed arrow), results in exsolution of pyrite from pyrrhotite with decreasing temperature.

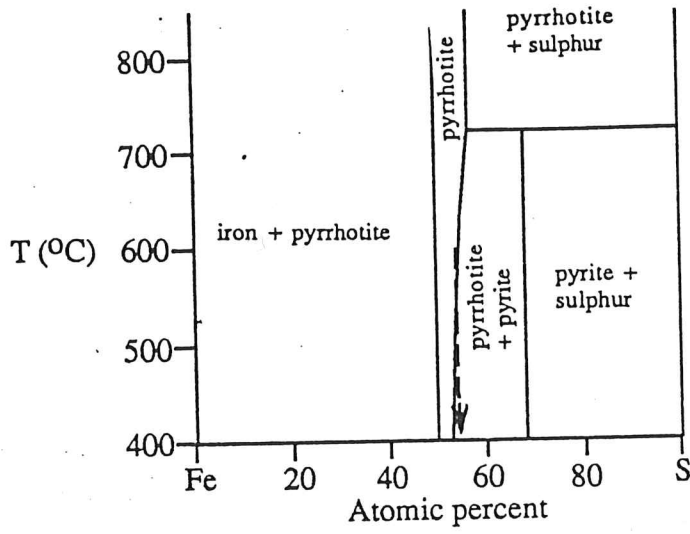
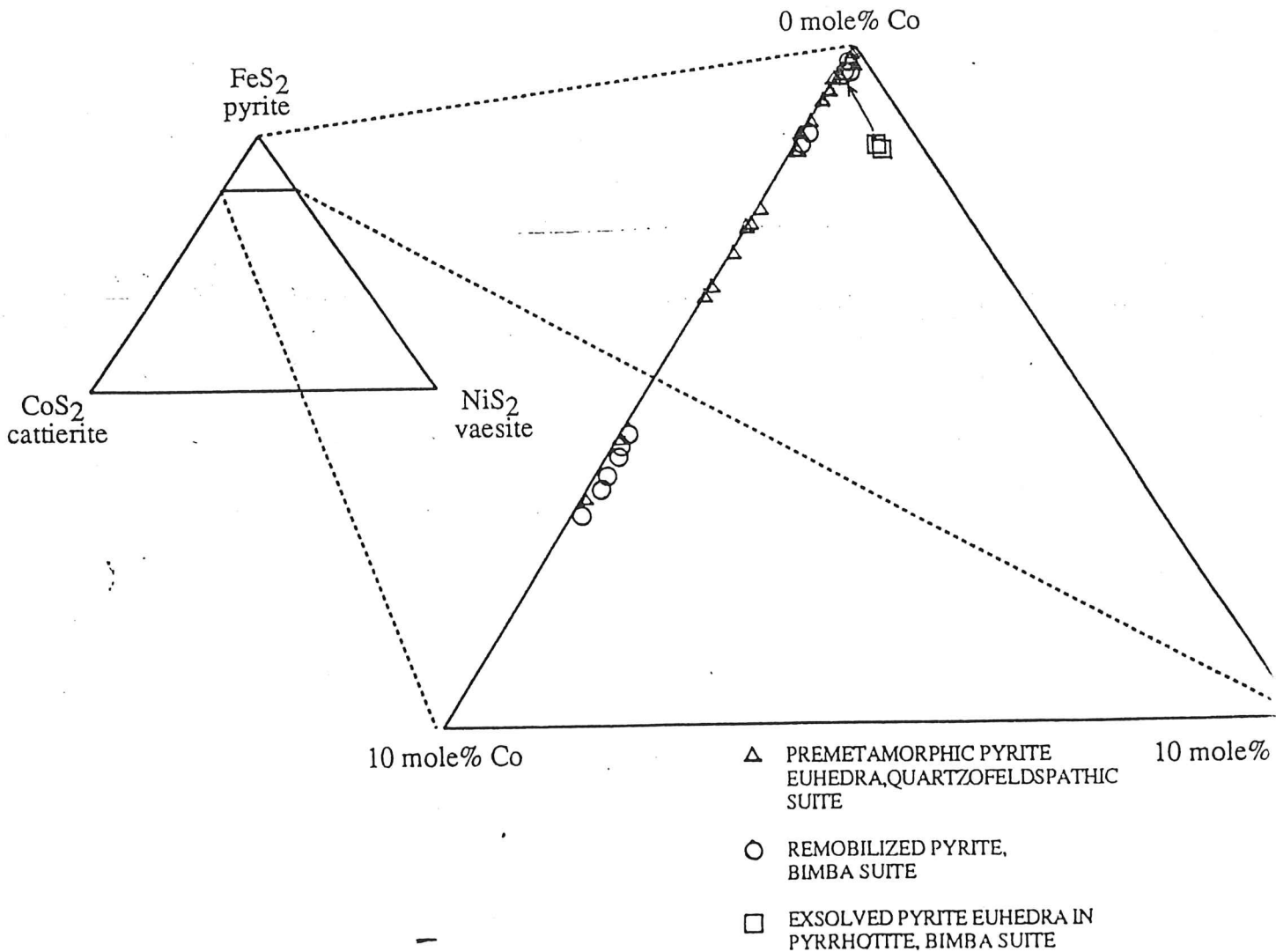


FIGURE (12): Plots of the compositions of Ethiudna pyrites onto a ternary diagram for the system  $\text{FeS}_2\text{-CoS}_2\text{-NiS}_2$ .





1964) and is indicative of precipitation from aqueous solution under conditions of varying cobalt and/or nickel activities. Preservation of zoning after heating to peak metamorphic temperatures is possible because of the high bond-strength and refractory nature of pyrite. Wheatley (1978), indicated that prolonged heating at temperatures in excess of 700°C is required to obliterate zoning in pyrite. Furthermore the solid-state diffusion process which acts to chemically homogenize the crystals could be severely retarded by the presence of the arsenic impurity atoms within the sulphide lattice (Putnis & McConnel, 1980).

(2) Remobilized pyrite present in the Bimba Suite (vide section 4.4) occurs as euhedral to subhedral disseminated grains associated with chalcopyrite and pyrrhotite. Such pyrites are characterized by relatively high cobalt contents and lack of zoning. Inclusions of chalcopyrite, Wollastonite Stage phases, and other peak metamorphic silicates are common (Plate 10) and are indicative of coeval crystallization with these phases. The presence of large (up to 15mm), euhedral, inclusion-free pyrite within marble layers of the Wollastonite-Diopside subunit, overgrown with euhedral chalcopyrite, pyrrhotite and quartz suggests precipitation of remobilized sulphide was locally more gradual, resulting in a clearly defined paragenesis.

(3) Small (<0.2mm), weakly cobaltian, euhedral pyrite crystals were commonly observed in anhedral pyrrhotite grains from both the Bimba and Quartzofeldspathic Suite (Plate 11). The lack of zoning and frequent parallel alignment of these crystals within the host pyrrhotite suggests they are an exsolution phase. Such exsolution results from the narrowing of the stability field of iron deficient pyrrhotite with decreasing temperature (Fig. 11; Craig, 1990). Preferential partitioning of Co into pyrite accounts for the observed Co-enrichment of the exsolved phase relative to the host (Vaughan & Craig, 1978).

CHALCOPYRITE: With the exception of the previously mentioned euhedral, marble-hosted assemblage, Ethiudna chalcopyrites occur as anhedral grains which locally attain 10mm in the Footwall Quartzite subunit. Analysis of chalcopyrites showed that trace amounts of zinc are

consistently present (up to 1600ppm), probably as a lattice impurity since no sphalerite inclusions were noted. Owing to its high malleability during deformation (McDonald, 1967) chalcopyrite is commonly observed intruded along grain boundaries of more brittle pyrite (Plate 9) and silicates. Leaching of iron by surface waters has locally resulted in the supergene replacement of chalcopyrite by chalcocite along grain boundaries and adjacent to fractures (Plate 12).

**PYRRHOTITE:** Pyrrhotites present in both the Bimba and Quartzofeldspathic Suite are indistinguishable both texturally and chemically. The origin of these pyrrhotites may be due to a) precipitation of Fe under conditions of low sulphur activity or, b) desulphidation of pyrite during prograde metamorphism according to the reaction



The latter mechanism is more probable for microclinolite-hosted sulphide since premetamorphic pyrite coexists with pyrrhotite in this setting. Direct textural evidence of replacement is lacking however. The lack of coevally crystallized pyrite and the association with low-sulphur phases such as skutterudite and cobaltite suggests the former mechanism is applicable to Bimba Suite pyrrhotites at the Ethiudna East prospect. Pyrrhotite grains are typically anhedral and commonly display curving of the prominent (001) cleavage suggestive of ductile deformation (Plate 13). Commonly late stage retrograde alteration to fine-grained pyrite/marcasite has occurred along grain boundaries and adjacent to fractures, indicative of partial iron removal by leaching (Craig, 1990) (Plate 13).

**MOLYBDENITE:** Rare laths of molybdenite were observed associated with cobaltian pyrite in both the Bimba and Quartzofeldspathic Suite (Plate 14). Deformation-imposed kinking of molybdenite laminae (Craig & Vaughan, 1981) was frequently observed.

SKUTTERUDITE/COBALTITE: Skutterudite is locally present in the Calc-Silicate Quartzite subunit at the Ethiudna East prospect, as anhedral disseminations to 10mm, frequently enclosing cobaltite euhedra (Plate 15). Inclusions of both chalcopyrite and bornite are common in both species, in apparent textural equilibrium as is evident by arcuate boundaries between phases (Plate 16). Brittle fracture of both skutterudite and cobaltite during deformation (Plate 15) has facilitated their oxidation to erythrite during the weathering process.

#### 4.3. DISTRIBUTION AND STRUCTURAL CONTROL OF MINERALIZATION: GENETIC IMPLICATIONS

The presence of the bulk of the sulphide mineralization as layers and beds parallel to compositional (sedimentary) layering in microclinolites of the Quartzofeldspathic Suite suggests mineralization has a syngenetic relationship to the deposition of this unit and is not, as previously suggested (Campana & King, 1958; Waterhouse, 1971), related to the intrusion of the Ethiudna Adamellite. This hypothesis is further supported by;

- a) the lack of skarn-features such as; abundant late-stage, sulphide-bearing cross-cutting veins, mineralization fronts proximal to intrusive contacts, and calc-silicate zoning in the overlying Bimba Suite. Such features are normally associated with mineralization accompanying intrusion of plutonic rocks into a calcareous unit (Einaudi et al., 1981).
- b) the regional occurrence of similar stratabound Cu-Co mineralization at the same stratigraphic level, in the absence of intrusive granitoids, eg. Mt. Howden (Michelmores, 1971), Meningie Well (Haas, 1980), Dome Rock (Ito & Plimer, 1987), and Thackaringa (Plimer, 1977).

No structural control of the microclinolite-hosted sulphides is evident in the study area, as would be expected if mineralization were emplaced during active deformation.

The case is less clear for sulphides in the overlying Bimba Suite owing to their sparsely disseminated nature. The major part of the sulphide mineralization in this unit throughout the study area is proposed as representing a peak metamorphic remobilization of microclinolite-hosted mineralization. Since the peak metamorphic event coincides with the major D2 folding event, some structural control of this mineralization is expected, especially since a metasomatic remobilization mechanism is inferred. The observed sulphide-gangue relationships suggest, however, that the localization of sulphides within the Bimba Suite is far more dependant on local calcite/calc-silicate to quartz (and feldspar) ratios within the suite, in keeping with the proposed chemical precipitation mechanism for such mineralization. Thus sulphide enrichments in the Bimba Suite are found to coincide with the development of the Wollastonite-Diopside subunit and carbonate-bearing or calc-silicate rich layers within the Footwall Quartzite and Calc-Silicate quartzite subunits. The late, Brittle-Fracture Stage of deformation is not associated with mineralization. Trace element analysis shows mesoscopic quartz veins and adjacent wallrock to be barren of mineralization, and microscopic quartz/calcite veins were commonly observed crosscutting preexisting sulphide grains.

#### 4.4. GENESIS OF STRATA-BOUND Cu-Co MINERALIZATION

Strata-bound and disseminated sulphide mineralization in the Quartzofeldspathic Suite at Ethiudna is proposed to be of the type known as a red-bed-associated Cu deposit. This genetic type is exemplified by the deposits of the Zambian and Zairean Copperbelts, White Pine (Michigan), and Dzhezkazgan (Kazakhstan), (Gustafson & Williams, 1981). The proposal is made on the basis of several geological, textural, and geochemical features shown by the Ethiudna mineralization which are characteristic of red-bed-associated Cu deposits, notably the predominance of Cu and Co, with negligible amounts of other ore metals (Gustafson &

Williams, 1981), together with the occurrence of the mineralization in predominantly clastic, feldspathic, hematitic (meta-) sediments (red-beds), and the close spatial association of (meta-) carbonate/evaporite beds and reduced carbonaceous pelites (Eugster, 1985).

Early theories on the genesis of this type of deposit which espoused an early diagenetic origin for Cu mineralization (Wedepohl, 1971), have lost favour in the light of petrographic and stratigraphic evidence, which indicates the metals were introduced into the sediments after early diagenesis (Ohmoto et al., 1990). These current theories postulate Cu (and Co) sulphides were formed by replacement of early diagenetic (biogenic) pyrite due to an influx of Cu, Co-bearing fluid after early diagenesis (Bartholomé et al., 1971; Brown, 1978; Ohmoto et al., 1990), and are based on the observed occurrence of authigenic chalcocite, chalcopyrite and euhedral cobaltian pyrite overgrowths on framboidal pyrite in these deposits. Textures identical to those described by Bartholomé et al. (1971), were observed in pyrite crystals from the Quartzfeldspathic Suite (viz; anhedral low-Co cores, probably the metamorphosed equivalent of framboids, overgrown with euhedral Co-rich pyrite; Plate 17), and are similarly interpreted to have formed due to late diagenetic influxes of Co-bearing fluids. Introduction of Cu is tentatively suggested to have occurred at the same time; the lack of chalcopyrite rims on pyrite being ascribed to the destruction of this textural association during metamorphism.

The sulphur isotope compositions of sulphides in the Quartzfeldspathic Suite (Fig.13), are similar to those of sulphides in stratabound Cu-Co deposits elsewhere in the OB, although  $\delta^{34}\text{S}$  distributions of sulphides from these other occurrences are typically centred on more negative values (-4‰; Cook & Ashley, 1992). Isotopic shifts to more positive  $\delta^{34}\text{S}$  values, induced by the depletion of  $^{32}\text{S}$  during the desulphidation of Ethudna sulphides (probably associated with intense high temperature Wollastonite Stage infiltrational metasomatism) are inferred to account for the difference. Such isotopic shifts are typically associated with fluid-present metamorphism of sulphides (Zheng, 1990). Narrow ranges of  $\delta^{34}\text{S}$  values in OB Cu-Co deposits are atypical of red-bed-associated Cu deposits (Gustafson

& Williams, 1981), and may reflect a relatively uniform sulphur source and depositional process (Cook & Ashley, 1992), or more likely the isotopic homogenizing effect of metamorphism (Zheng, 1990), which has affected all these deposits.

#### 4.5. EVIDENCE FOR METASOMATIC REMOBILIZATION OF MINERALIZATION

Sulphide mineralization in the Bimba Suite is suggested as representing a chemical remobilization of mineralization from the underlying Quartzofeldspathic Suite, a hypothesis based on several lines of geochemical and petrological evidence. This remobilization of ore elements and sulphur is proposed to have occurred during infiltrational metasomatism associated with the petrogenesis of the Bimba Suite.

The observed textural equilibrium between Bimba Suite sulphides and Wollastonite-Stage assemblages and other peak metamorphic phases suggests that remobilization took place during metasomatism associated with the Wollastonite Stage. No textural evidence exists to suggest any significant remobilization occurred during the retrograde Grossular Stage infiltrational episode, or the later Brittle-Fracture Stage.

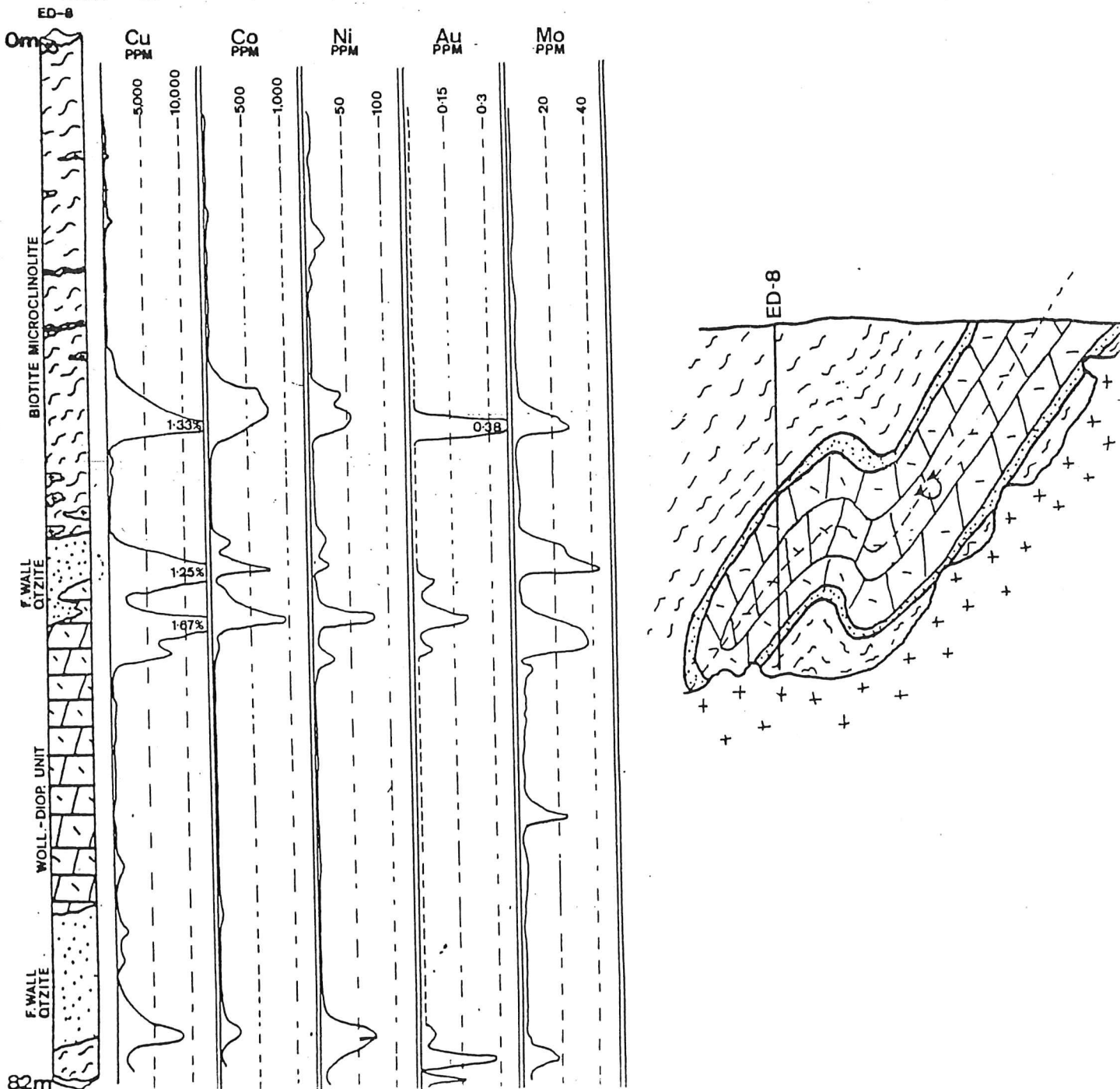
Differences between the geochemistry of Bimba Suite mineralization and that of the inferred parent microclinolite-hosted mineralization are marked. Bimba Suite mineralization is characterized by higher Cu:Fe, Co:Fe, As:S ratios, and higher absolute concentrations of Au and Mo (Table 5). These differences, similar examples of which have been documented from other deposits in which metasomatic ore remobilization has been implicated, (Mookherjee, 1976), are suggested as being a reflection of the higher solubilities of Cu, Co, As, Au and Mo in the metasomatic fluid relative to Fe and S. Preferential leaching and transport of these elements from the parent ore, would have been facilitated by the high Cl-content of the metasomatic fluids (as previously demonstrated), which would promote Cl-complexing of metals such as Cu and Co (Barnes & Czamanske, 1967), as well as the high  $fO_2$  of the fluids

TABLE (5): Geochemical characteristics of Ethjudna mineralization

(SUB-)UNIT	Cu:Fe	Co:Fe	S:As	Au (max.)	%Co in Pyrite		
					average	max.	min.
Wollastonite-Diopside	v. high	high	high	0.20 ppm	0.55	1.98	0.04
Footwall Quartzite	high to v. high	v. high	high	0.40 ppm	6.42	7.08	5.94
Calc-Silicate Quartzite	high	v. high	low	—	—	—	—
Quartzofeldspathic	low	low	v. high	0.38 ppm	1.09	6.45	0.05

— not measured

FIGURE (14): Drill-hole assay profiles for Cu, Co, Ni, Au and Mo, from drill core ED-8, Ethjudna mines.





(assuming they had previously equilibrated with the hematite-bearing microclinolites), (Barnes & Czamanske, 1967).

The localization of Bimba Suite mineralization to calcite and/or calc-silicate-rich lithologies supports the suggestion that destabilization of metal complexes, and subsequent precipitation of metals was effected by a pH rise, induced by reaction of metasomatic fluids with carbonates. This concept of the carbonate-rich Bimba Suite acting as a chemical trap for mobilized ore elements during metamorphism is supported by drill hole assay evidence; drill hole assay profiles show large increases in the absolute concentrations of Cu, Co, Ni, Au, and Mo in the Footwall Quartzite and Wollastonite-Diopside subunits proximal to the Bimba/Quartzofeldspathic Suite contact (Fig. 14). The lack of primary sulphide mineralization in, or adjacent to, the highly reduced graphitic pelites of the Pelite Suite, suggests changes in the  $fO_2$  were probably not instrumental in the precipitation of mobilized metals.

The source of sulphur required for the precipitation of ore elements as sulphides, is suggested to be that released into the infiltrating fluids during the metamorphic desulphidation of pyrite (vide section 4.2). Low sulphur assemblages in the Bimba Suite are suggested to have formed as a result of locally depressed  $\delta^{34}S$  of depositing metasomatic fluids. The identical sulphur isotope signature of Bimba Suite and Quartzofeldspathic Suite sulphides (Fig. 13) reflects their genetic link, and/or the isotopic-homogenizing effect of infiltrating fluids (Zheng, 1990).

## CHAPTER 5 : SUMMARY

The development of Wollastonite Stage and Grossular Stage assemblages in the Bimba Suite at Ethiudna reflects two discrete episodes of fluid infiltration. Wollastonite Stage assemblages, which contain amphibolite-facies phases such as diopside and wollastonite, are suggested to have developed during prograde amphibolite facies metamorphism ( $P < 4\text{ kbars}$ ,  $T < 600^\circ\text{C}$ ), which was coeval with the Olarian D2 deformational episode. The Wollastonite Stage of petrogenesis was associated with intense, and pervasive infiltrational metasomatism. Infiltrating fluids were  $\text{H}_2\text{O}$ -rich ( $X_{\text{CO}_2} < 0.18$ ),  $\text{NaCl}$ -bearing, and probably isotopically equilibrated (in terms of oxygen isotopes) with siliciclastics. Pervasive infiltration of the Wollastonite-Diopside subunit is suggested to have been effected by the development of a reaction enhanced permeability.

Grossular Stage assemblages were developed during a second infiltrational episode at lower (retrograde metamorphic) temperatures ( $\sim 300^\circ\text{C}$ ). Infiltrating fluids were focussed along structurally-induced zones of high permeability. Development of the characteristic Grossular Stage assemblage, grossular-quartz, occurred as a result of metasomatic depletion of  $\text{K}_2\text{O}$  in the Wollastonite Stage assemblage, wollastonite-microcline. Variations in fluid/rock ratios resulting from heterogeneous fluid flow during this stage, are suggested to account for the observed marked variation in the progress of the grossular-quartz producing reaction. Grossular Stage infiltrating fluids were essentially  $\text{CO}_2$ -free, and highly saline, containing  $\text{CaCl}_2$ ,  $\text{NaCl}$ , and other electrolyte species.

The formation of Brittle-Fracture Stage quartz veins postdates both the Wollastonite Stage and Grossular Stage. These veins were probably deposited by low temperature ( $< 250^\circ\text{C}$ ), saline fluids, which permeated fractures formed during a late-stage deformation event.

The stratiform nature of Cu-Co mineralization in the Quartzofeldspathic Suite is consistent with the suggestion that the deposition of this mineralization is syngenetic with the sedimentation/diagenesis of the unit. Geochemical and petrological evidence suggests this mineralization is of the genetic type known as a red-bed-associated Cu deposit. The distribution, geochemistry, and textural characteristics of sulphides in the Bimba Suite suggests this mineralization represents a metasomatic remobilization of stratabound mineralization present in the underlying Quartzofeldspathic Suite.

## REFERENCES

- Ashley, P.M., (1984), Sodic granitoids and felsic gneisses associated with uranium-thorium mineralization, Crocker's Well, South Australia; *Mineralium Deposita*, **19**, pg.7-18.
- Barnes, H.L., Czamanske, G.K., (1967), Solubilities and transport of ore minerals; in *Geochemistry of Hydrothermal Ore Deposits*; Holt, Rinehart and Winston Inc., New York, pg.335-378.
- Bartholomé, P., Katekesha, F., (1971), Cobalt zoning in microscopic pyrite from Kamoto, Republic of the Congo (Kinshasa); *Mineralium Deposita*, **6**, pg.167-176.
- Bickle, M.J., Baker, J., (1990), Advective-diffusive transport of isotopic fronts: an example from Naxos, Greece; *Earth and Planetary Science Letters*, **97**, pg.78-93.
- Bickle, M.J., McKenzie, D., (1987), The transport of heat and matter by fluids during metamorphism; *Contributions to Mineralogy and Petrology*, **95**, pg.384-392.
- Both, R.A., Rutland, R.W.R., (1976), The problem of identifying and interpreting stratiform ore bodies in highly metamorphosed terrains: the Broken Hill example; in *Handbook of Strata-bound and Stratiform ore deposits*, **4**, Elsevier, Amsterdam, pg.261-325.
- Brown, A.C., (1978), Stratiform copper deposits-evidence for their post-sedimentary origin; *Mineral Science and Engineering*, **10**, 172-181.
- Campana, B., King, D., (1958), *Regional Geology and mineral resources of the Olary Province*; Geological Survey of South Australia, Bulletin 34, 133pp.
- Chappel, B.W., White, A.R.J., (1974), Two contrasting granite types; *Pacific Geology*, **8**, pg. 173-174.
- Clarke, G.L., Burg, J.P., Wilson, C.J.L., (1986), Stratigraphic and structural constraints on the Proterozoic tectonic history of the Olary Block, South Australia; *Precambrian Research*, **34**, pg.107-137.

- Clarke, G.L., Guiraud, M., Powell, R., Burg, J.P., (1987), Metamorphism in the Olary Block, South Australia: compression with cooling in a Proterozoic fold belt; *Journal of Metamorphic Geology*, **5**, pg.291-306.
- Cook, N.D.J., Ashley, P.M., (1992), Meta-evaporite sequence, exhalative chemical sediments and associated rocks in the Proterozoic Willyama Supergroup, South Australia: implications for metallogenesis; *Precambrian Research*, **56**, pg.211-226.
- Coombs, D.S., (1965), Sedimentary analcime rocks and sodium-rich gneisses; *Mineralogical Magazine*, **54**, pg.144-159.
- Craig, J.R., (1990), Textures of the ore minerals; in *Short Course on Advanced Microscopic Studies of Ore Minerals*, Mineralogical Society of Canada, pg.213-256.
- Craig, J.R., Vaughan, D.J., (1981), *Ore Microscopy and Ore Petrography*; Wiley, New York, 405pp.
- Crawford, M.L., (1981a), Phase equilibria in aqueous fluid inclusions; in *Short Course in Fluid Inclusions: Applications to Petrology*, Mineralogical Society of Canada, pg. 75-97.
- Crawford, M.L., (1981b), Fluid inclusions in high grade metamorphic rocks; in *Short Course in Fluid Inclusions: Applications to Petrology*, Mineralogical Society of Canada, pg.182-204.
- Einaudi, M.T., Meinert, L.D., Newberry, R.J., (1981), Skarn deposits; *Economic Geology, 75th Anniversary Volume*, pg.317-396.
- Ellis, D.E., (1978), Stability and phase equilibria of chloride and carbonate bearing scapolite at 750°C and 4000bars; *Geochimica et Cosmochimica Acta*, **42**, pg. 1271-1280.
- Eugster, H.P., (1985), Oil shales, evaporites and ore deposits; *Geochimica et Cosmochimica Acta*, **49**, pg.619-635.

- Floyd, P.A., Winchester, J.A., (1978), Identification and discrimination of altered and metamorphosed volcanic rocks using immobile elements; *Chemical Geology*, **21**, pg.291-306.
- Golding, S.D., Clark, M.E., Keele, R.A., Wilson, A.F., Keays, R.R., (1985), Geochemistry of Archean epigenetic gold deposits in the Eastern Goldfields Province, Western Australia; in *Stable Isotopes and Fluid Processes in Mineralization*, University of Western Australia Publication No.23, pg.141-176.
- Greenwood, H.J., (1967), Wollastonite: stability in H<sub>2</sub>O-CO<sub>2</sub> mixtures and occurrence in a contact metamorphic aureole near Salmo, British Columbia, Canada; *American Mineralogist*, **52**, pg.1669-1680.
- Gustafson, L.B., Williams, N., (1981), Sediment-hosted stratiform deposits of copper, lead and zinc; *Economic Geology, 75th Anniversary Volume*, pg.139-178.
- Haas, L., (1980), A study of the pyrite-calc-silicate relationship in the Meningie Well area, Olary Province; Honours thesis, University of Adelaide, unpublished.
- Ito, T., Plimer, I.R., (1987), The significance of tourmaline in the stratiform Dome Rock deposit, Australia; *Mining Geology*, **37**, pg.403-418.
- Lawrence, L.J., (1972), The thermal metamorphism of a pyritic sulfide ore; *Economic Geology*, **67**, pg.487-496.
- Leah, P.A., (1985), Petrology, structure, and stratigraphy of the Willyama Supergroup and Olarian granitoids, west of Plumbago Homestead, Olary Block, South Australia; Honours thesis, University of Adelaide, unpublished.
- Levien, L., Papike, J.J., (1976), Scapolite crystal chemistry: aluminium-silicon distribution, carbonate group disorder, and thermal expansion; *American Mineralogist*, **61**, pg.864-877.
- McDonald, J.A., (1967), Metamorphism and its effect on sulphide assemblages; *Mineralium Deposita*, **2**, pg.200-220.

- Michelmore, T.R., (1971), The geology of copper mineralized areas in the Olary Province; Honours thesis, University of Adelaide, unpublished.
- Mookherjee, A., (1976), Ores and metamorphism: temporal and genetic relationships; in *Handbook of Strata-bound and Stratiform ore deposits*, 4, Elsevier, Amsterdam, pg.203-251.
- Ohmoto, H., Kaiser, C.J., Geer, K.A., (1985), Systematics of sulphur isotopes in recent marine sediments and ancient sediment-hosted basemetal deposits; in *Stable Isotopes and Fluid Processes in Mineralization*, University of Western Australia Publication No.23, pg.70-121.
- Oliver, N.H.S., Valenta, R.K., Wall, V.J., (1990), The effect of heterogeneous stress and strain on metamorphic fluid flow, Mary Kathleen, Australia, and a model for large-scale fluid circulation; *Journal of Metamorphic Geology*, 8, pg.311-331.
- Oliver, N.H.S., Wall, V.J., Cartwright, I., (1992), Internal control of fluid composition in amphibolite-facies scapolite calc-silicates, Mary Kathleen, Australia; *Contributions to Mineralogy and Petrology*, 111, pg.94-112.
- Oliver, N.H.S., Wall, V.J., Golding, S.D., (1990), Heterogeneous fluid flow in polydeformed calc-silicates of the Mary Kathleen Fold Belt, Queensland, Australia; in *Stable Isotopes and Fluid Processes in Mineralization*, University of Western Australia Publication No.23, pg.141-176.
- Orville, P.M., (1975), Stability of scapolite in the system Ab-An-NaCl-CaCO<sub>3</sub> at 4kbar and 750°C; *Geochimica et Cosmochimica Acta*, 39, pg.1091-1105.
- Plimer, I.R., (1977), The origin of albite-rich rocks enclosing the cobaltian pyrite deposit at Thackaringa, N.S.W., Australia; *Mineralium Deposita*, 12, pg.175-187.
- Putnis, A., McConnell, J.D.C., (1980), *Principles of Mineral Behavior*; Blackwell, Oxford, 342pp.
- Ramdohr, P., (1969), *The Ore Minerals and their Intergrowths*, Pergamon, Oxford, 1174pp.







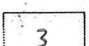

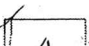





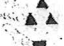

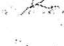

- Rice, J.M., Baker, J., (1982), Buffering, infiltration, and the control of intensive variables during metamorphism; in *Characterization of Metamorphism through Mineral Equilibria; Reviews in Mineralogy*, **10**, Mineralogical Society of America, pg.263-324.
- Robinson, B.W., Kusakabe, M., (1975), Quantitative preparation of sulphur dioxide for  $^{34}\text{S}/^{32}\text{S}$  analysis, from sulphides by combustion with cuprous oxides; *Analytical Chemistry*, **47**, pg.1179-1181.
- Schenk, V., (1984), Petrology of felsic granulites, metapelites, metabasics, ultramafics, and metacarbonates from southern Calabria (Italy): prograde metamorphism, uplift and cooling of a former lower crust; *Journal of Petrology*, **25**, pg.255-298.
- Slack, J.F., Palmer, M.R., Stevens, B.P.J., (1989), Boron isotope evidence for the involvement of non-marine evaporites in the origin of the Broken Hill ore deposits; *Nature*, **342**, pg.913-916.
- Springer, G., Schachner-Korn, D., Long, J.V.P., (1964), Metastable solid solution relations in the system  $\text{FeS}_2\text{-CoS}_2\text{-NiS}_2$ ; *Economic Geology*, **59**, pg.475-491.
- Stanton, R.L., (1972), *Ore Petrology*; McGraw-Hill, New York, 713pp.
- Stevens, B.P.J., Stroud, W.J., Willis, I.L., Bradley, G.M., Brown, R.E., Barnes, R.J., (1980), A stratigraphic interpretation of the Broken Hill Block; in *A Guide to the Stratigraphy and mineralization of the Broken Hill Block, N.S.W.*; N.S.W. Geological Survey Records, **20**, pg.9-32.
- Surdam, R.C., Parker, R.D., (1972), Authigenic aluminosilicate minerals in the tuffaceous rocks of the Green River Formation, Wyoming; *Geological Society of America, Bulletin* **83**, pg.689-700.
- Taylor, H.P., (1979), Oxygen isotope studies of hydrothermal mineral deposits; in *Geochemistry of Hydrothermal Ore Deposits*; Holt, Rinehart and Winston Inc., New York, pg.109-140.

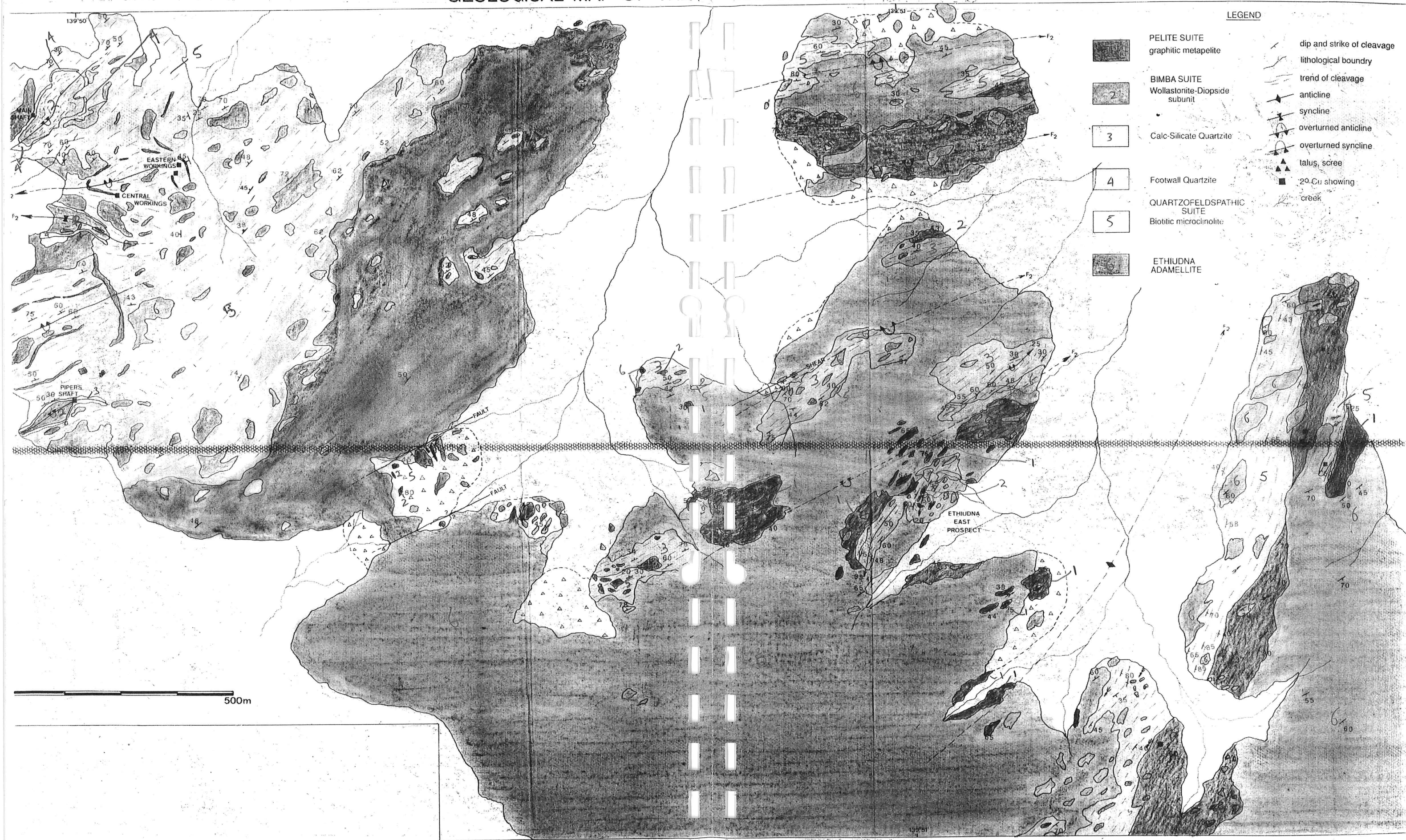
- Valley, J.W., (1986), Stable isotope geochemistry of metamorphic rocks; in *Stable Isotopes in High Temperature Geological Processes; Reviews in Mineralogy*, **16**, Mineralogical Society of America, pg.445-486.
- Vanko, D.A., Bishop, F.C., (1980), Experimental determination of NaCl-rich scapolite stability; *Geological Society of America, Abstracts with Programs*, **12**, pg.540.
- Vaughan, D.J., Craig, J.R., (1978), *Mineral Chemistry of Metal Sulphides*; Cambridge University Press, 493pp.
- Waterhouse, J.D., (1971), The geology of the Ethudna and Walparuta Mine areas, Olary Province, South Australia; Honours thesis, University of Adelaide, unpublished.
- Wedepohl, K.H., (1971), "Kupferschiefer" as a prototype of syngenetic sedimentary ore Deposits; *Society of mining Geologists Japan Special Issue*, **3**, pg.268-273.
- Wheatley, C.J.V., (1978), Ore mineral fabrics in the Avoca polymetallic sulphide deposit, south-east Ireland; in *Mineralization in Metamorphic Terrains, Geological Survey of South Africa, Special Publication No.4*, pg.529-544.
- Willis, I.L., Brown, R.E., Stroud, W.J., Stevens, B.P.J., (1983), The early Proterozoic Willyama Supergroup: stratigraphic subdivision and interpretation of the high to low grade metamorphic rocks in the Broken Hill Block, New South Wales; *Journal of the Geological Society of Australia*, **30**, pg.195-224.
- Zheng, Y.F., (1990), Sulfur isotopes in metamorphic rocks; *Neues Jahrbuch für Mineralogie, Abhandlungen*, **161**, pg.303-325.



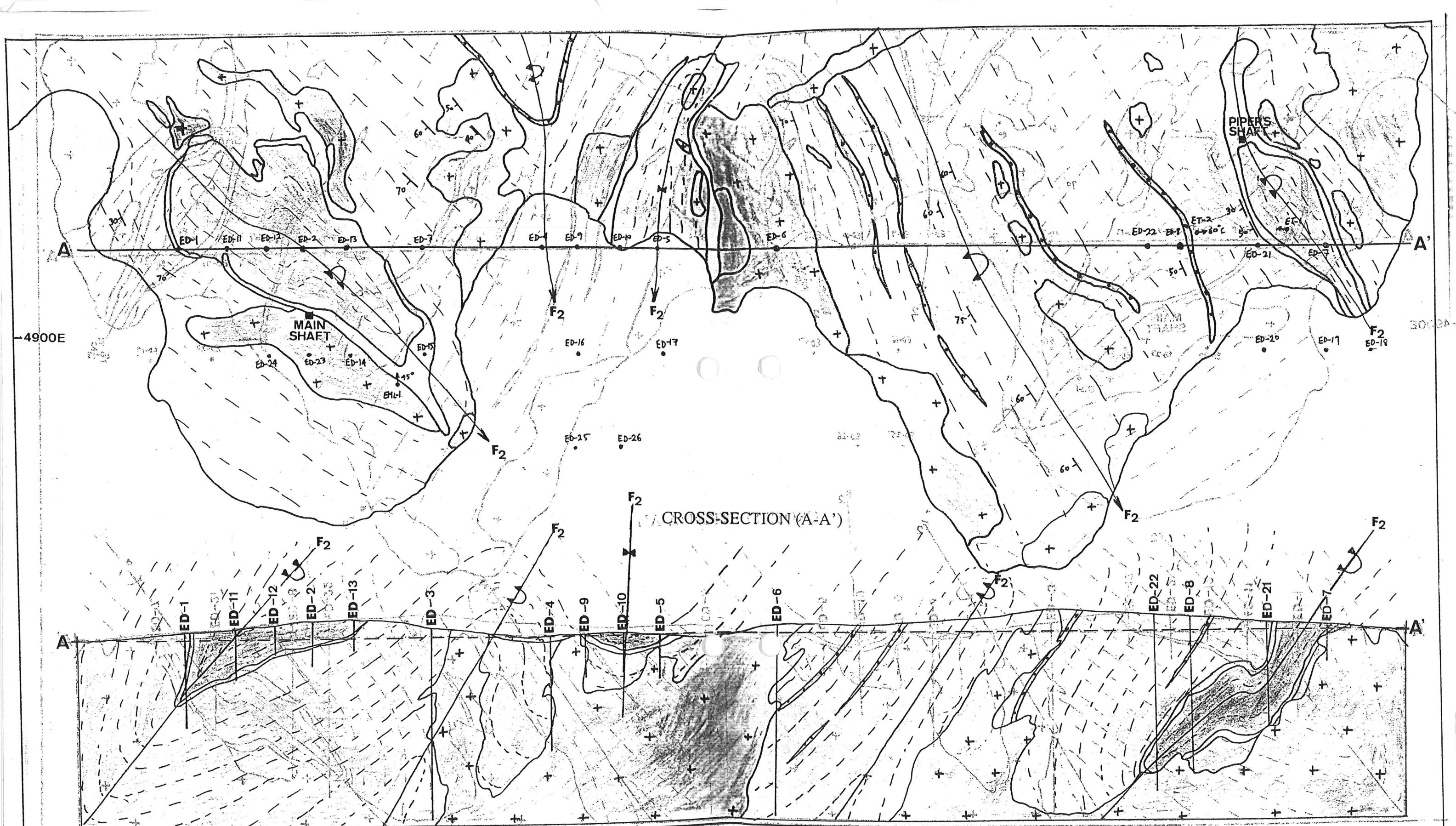
# GEOLOGICAL MAP OF THE ETHIUDNA AREA

## LEGEND

- |   |  |   |                            |
|---|--|---|----------------------------|
|  | PELITE SUITE<br>graphitic metapelite                     |  | dip and strike of cleavage |
|  | BIMBA SUITE<br>Wollastonite-Diopside subunit             |  | lithological boundary      |
|  | 3<br>Calc-Silicate Quartzite                             |  | trend of cleavage          |
|  | 4<br>Footwall Quartzite                                  |  | anticline                  |
|  | 5<br>QUARTZOFELDSPATHIC SUITE<br>Biotitic microclinolite |  | syncline                   |
|  | ETHIUDNA<br>ADAMELLITE                                   |  | overturned anticline       |
|   |  |  | overturned syncline        |
|   |  |  | talus, scree               |
|   |  |  | 20 Cu showing              |
|   |  |  | creek                      |







DETAILED GEOLOGY OF THE ETHIUNDA MINES

AREA

WOLLASTONITE-DIOPSIDE SUBUNIT	ETHIUNDA ADAMELLITE	alluvium	dip/strike of cleavage
FOOTWALL QUARTZITE	pelite interbed	trend of cleavage	diamond drill hole
BIOTITE MICROCLINOLITE			

DETAILED GEOLOGY OF THE ETHIUNDA MINES

100M

4800M

M.N.

T.N.

ETHIUNDA ADAMELLITE	ETHIUNDA ADAMELLITE	alluvium	dip/strike of cleavage
FOOTWALL QUARTZITE	pelite interbed	trend of cleavage	diamond drill hole
BIOTITE MICROCLINOLITE			

PLATES 1 to 6 illustrate the marked variation in the development of Grossular Stage assemblages as replacements of the Wollastonite Stage microcline-wollastonite association.

- PLATE 1: Wollastonite-rich layers of the Wollastonite-Diopside subunit in a section of drill core (ED-23), from the Ethiudna mines. Note layered fabric defined by diopside porphyroblasts (dark-green). Grossular Stage phases are absent.
- PLATE 2: Photomicrograph (in plane polarized light) showing textural equilibrium between phases of the Wollastonite-Stage assemblage, wollastonite (wo)- diopside (di) - microcline (ksp), in the Wollastonite-Diopside subunit, Ethiudna mines. Development of Grossular Stage phases as replacements of coexisting wollastonite and microcline has not occurred. Note accessory titanite (ti).
- PLATE 3: Partial replacement of Wollastonite Stage, prismatic, wollastonite by Grossular Stage grossular (gr) and quartz (not visible), on a macroscopic scale. Wollastonite-Diopside subunit, Ethiudna East prospect.
- PLATE 4: Photomicrograph showing development of a grossular+quartz (gr + qtz) rim between Wollastonite Stage microcline and wollastonite, indicating partial replacement of these two earlier-developed phases. Wollastonite-Diopside subunit, Ethiudna mines.(Plane polarized light).
- PLATE 5: Essentially pure grossular-quartz rock present in the hinge of a F2 fold in the Wollastonite-Diopside subunit at the Ethiudna East prospect. Lack of wollastonite and presence of trace microcline implies 100% progress of reaction (2), (vide text).
- PLATE 6: Photomicrograph (in plane polarized light) showing textures of grossular-quartz rock in Plate 5 on a microscopic scale. Trace microcline (ksp) is rimmed by Grossular Stage grossular and quartz (gr + qtz), which in the top right corner of the plate are present as pseudomorphs after prismatic wollastonite.



